北海道工業開発試験所報告

REPORTS OF THE GOVERNMENT INDUSTRIAL DEVELOPMENT LABORATORY, HOKKAIDO

第46号　　昭和63年3月

目　　次

工業技術院
北海道工業開発試験所

酸素と水蒸気による石炭と石炭チャーの流動層ガス化

田崎米四郎，千葉　繁生，弓山　　翠，本間　専治
北野　邦尋，武田　詔平，河端　淳一，鈴木　　智

1. 緒　　言

石炭から合成原料ガスを製造する場合，ガス化剤には酸素と水蒸気が使用される。一般的には酸素濃度の増加と共にガス化温度も高くなり[1]，灰の融点以上の高温で行われる気流層ガス化の場合には，純酸素が使われることもある[2]。流動層ガス化方式のように灰をドライな状態で取り出す場合には，クリンカーが生成しないようにすることが必要で，酸素濃度に制限があり，通常水蒸気で希釈する[3]。

本研究は，太平洋炭及び，太平洋炭を500℃で流動乾留したチャーを使用して，常圧流動層ガス化におけるガス化剤中の酸素濃度の限界を知ること，及び酸素濃度が生成ガス組成に与える影響を調べることを目的とするものである。

2. 常圧ガス化実験装置及び方法

常圧ガス化フローの概略をFig. 1に示す。流動層ガス化炉本体は内径0.108mϕ，全長1.15mのSUS−32製で，目皿は穴径2㎜，開孔比2％のSUS−42製のものを使用した。オーバーフローは目皿より0.4mの高さとした。ガス化試料は，Table 1に示したものである。

Table 1. Chemical analysis and physical properties of materiales used

	Taiheiyo coal (TC)	500℃char (TCC)
Proximate analysis (wt%)		
Moisture	4.7	2.6
Ash	16.5	24.3
Volatile matter	44.9	20.2
Fixid carbon	34.2	52.9
Ultimate analysis (d.f.wt%)		
C	65.0	60.4
H	5.4	3.0
O	13.1	9.5
N	1.0	1.3
S	0.3	0.3
Ash	15.1	25.5
High heating value (cal／g)	6080	5420

	Taiheiyo coal	500℃ char	Silica sand
d_p (㎜)	0.35−2.00	−2.00	0.35−0.50
U_{mf} (m／s)	0.22	0.15	0.34

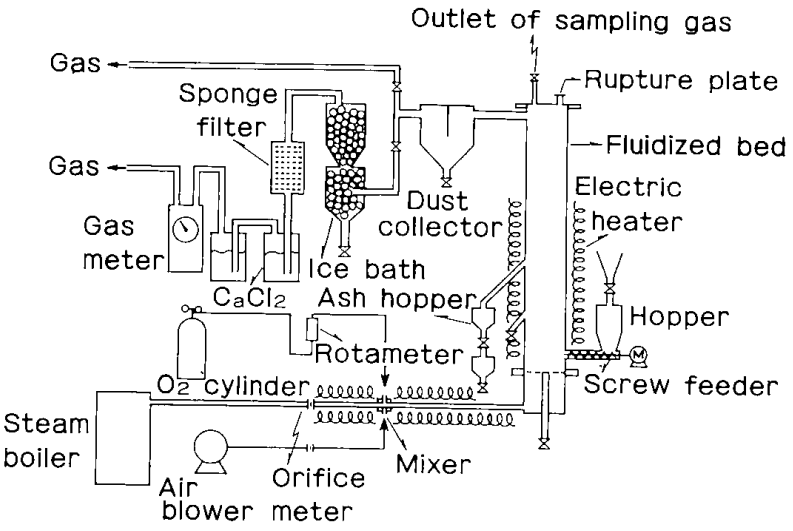

Fig. 1 Schematic diagram of experimental apparatus.

実験は，① Silica Sand （SS） 2 kgをあらかじめ炉内に投入し，太平洋炭（TC）をガス化試料として用いた場合，② 同じ条件で太平洋炭500℃チャー（TCC）をガス化試料とした場合，③ Silica Sandを用いず太平洋炭500℃チャーをガス化試料とした場合の３条件について行った。

炉内温度T_bは1,000℃とした。温度制御は設定した炉内温度を一定に保つように，供給する試料の量を増減する供給量制御方式で行った。

実験方法は，次の通りである。石炭もしくは石炭チャーを供給しつつ空気と水蒸気によって流動化し，炉内温度を上昇させ，800℃になったところで昇温用の外熱ヒーターを切る。さらに，石炭もしくは石炭チャーの部分燃焼により，900℃まで昇温させた時点で，空気の供給を停止し酸素を吹き込み，酸素と水蒸気をガス化剤として1,000℃でガス化した。炉内ガス流速は0.57m／sec（室温換算）とした。

発生ガスは，集塵器を通過させた後，氷を入れた容器に導入し，未反応水蒸気とダストを除去した。さらに，スポンジ状のフィルターとスチールウール層を通してタールを除去した。最後に，塩化カルシウムによって完全に除湿してからガス流量を測定した。

3. 実験結果及び考察

クリンカーが発生しない場合には流動状態が安定であり，流動層内はFig. 2に示すように均一な温度となる。しかし，クリンカーが発生すると，流動状態は不安定となって，Fig. 3に示すように層内に温度差が生じ，ついには流動化が停止する。

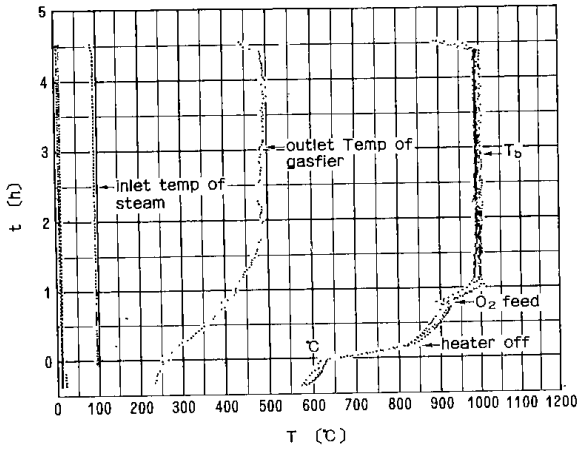

Fig. 2 Typical temperature profiles in the fluidized bed gasifier.

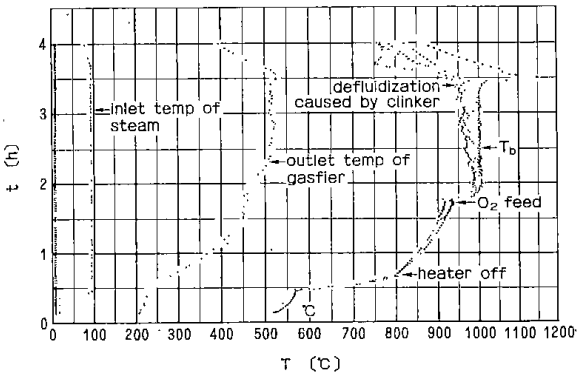

Fig. 3 The variation of temperatures with sintering of coal ash.

Fig. 4に流動が安定な状態におけるガス化剤中の酸素濃度と石炭もしくは石炭チャー供給量Fとの関係を示した。ガス化温度は，試料の供給量によって制御されるため，酸素濃度が高くなるに従って供給量Fは多くなる。

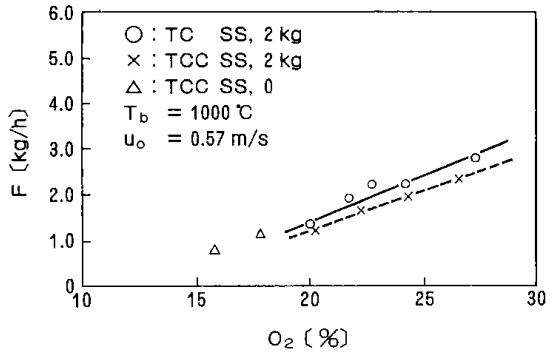

Fig. 4 Effect of oxygen concentration on the fuel feed rate.

次に，ガス化成績を評価するために諸効率を以下のように定義する。

Carbon conversion C_C（炭素効率）

$$C_C=\frac{\text{(生成ガス中のCO, } CH_4 \text{ 中の炭素)}}{\text{(供給TC, TCC中の炭素)}}$$

Carbon gasified C_g（炭素ガス化率）

$$C_g=\frac{\text{(生成ガス中のCO, } CH_4, CO_2 \text{ 中の炭素)}}{\text{(供給TC, TCC中の炭素)}}$$

Figs. 5，6は太平洋炭，Figs. 7，8は石炭チャーについてのC_C，C_g及び，生成ガス組成を示しており，いずれの場合もSilica Sandを流動媒体として使用している。これらの結果によるとC_gの値

はほぼ一定であるが，C_cの値，COとH_2ガス濃度及び生成ガス発熱量H_hは酸素濃度の増加と共に増大することを示している。又，石炭チャーの場合のC_c，C_gは石炭の場合のそれより大きいが，これは，石炭の場合，タール分として除かれる炭素が多いためと考えられる。しかし，生成ガス発熱量は，メタン濃度の相違によって，石炭の場合の方が大きくなっている。

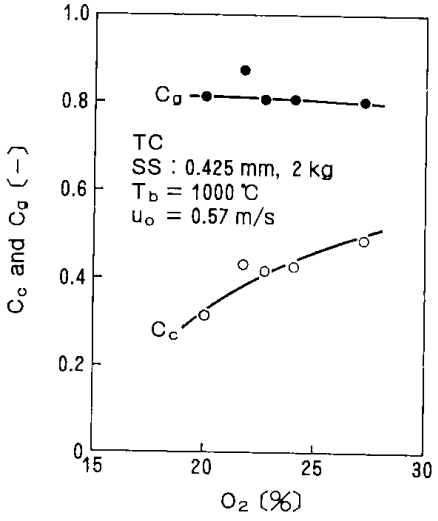

Fig. 5 Effect of the oxygen concentration on C_c and C_g for Taiheiyo coal.

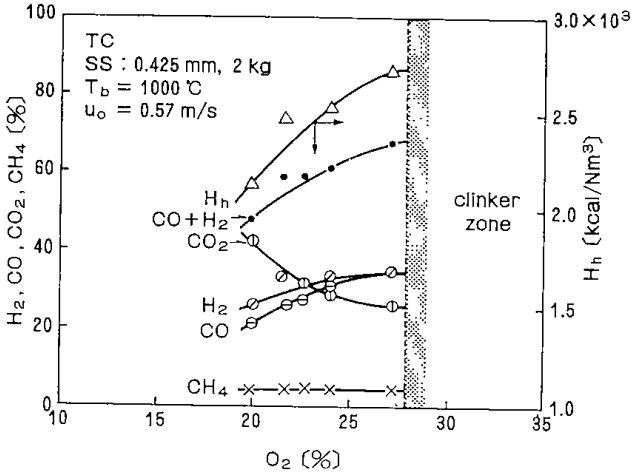

Fig. 6 Effect of varying the oxygen concentration for Taiheiyo coal.

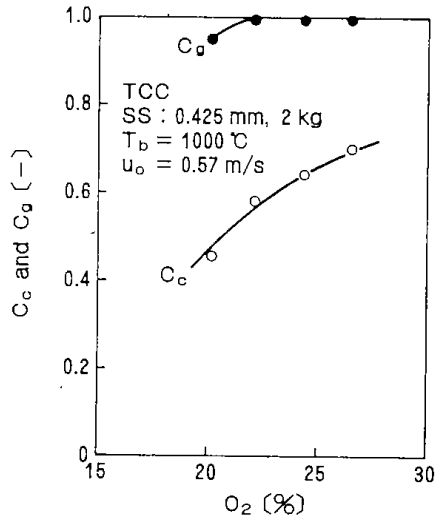

Fig. 7 Effect of the oxygen concentration on C_c and C_g for Taiheiyo coal char.

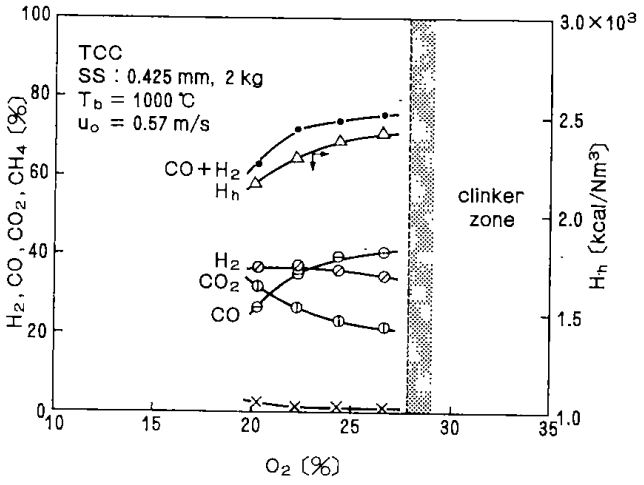

Fig. 8 Effect of varying the oxygen concentration for Taiheiyo coal char.

Figs. 6，8に示すように，炉内温度が1,000℃でSilica Sandを流動媒体として使用した場合，酸素濃度が約28%まではクリンカーは生成しなかったが，さらに，高酸素濃度領域では石炭及び石炭チャーを問わずクリンカーが発生し，流動状態を維持できなかった。

石炭チャーについて，Silica Sandを使用しない場合のC_c，C_g及びクリンカー生成域を求め，Fig. 8の結果と合わせてFig. 9に示した。Silica Sandを使用しない時は，酸素濃度が約18%でクリンカーが生じ実験は不可能となった。Fig. 9によると酸素濃度が17%ではH_2：CO＝2：1となり，メタノール合成に適したガス組成になる。23%位ではH_2：CO＝1：1になり，さらに，高酸素濃

度領域においては，CO濃度はH_2濃度より高くなる。従って，ある範囲内では酸素濃度によって取得するガス組成を制御することが出来る。

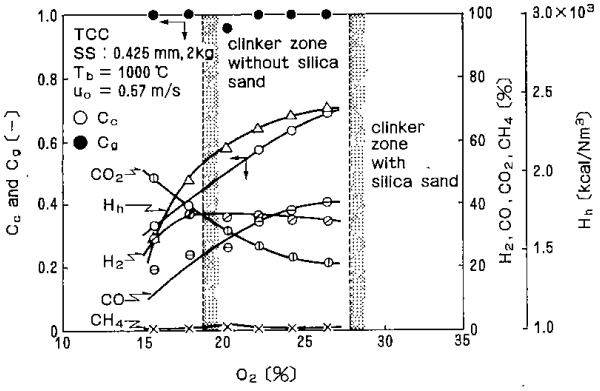

Fig. 9 Effects of feed oxygen concentration and inert silica sand particles on sintering of Taihelyo coal char.

4. まとめ

常圧流動層ガス化において炉内温度を1,000℃一定とし，クリンカーの生成及びガス組成に与える酸素濃度の影響を調べた。

このガス化法は，装置の運転も容易で，供給量制御方式のために残存酸素が炉内の上部に入り爆発する危険性も少なく安全である。クリンカー生成域外におけるガス化では，H_2及びCOが65～70％の比率を占め，CO_2除去後のカロリーは約4,000 kcal／N㎥ になる。このことから中カロリーガス，直接製鉄用還元ガス，合成用原料ガス等としての使用も可能である。

謝　辞

本報告をまとめるにあたり，富田稔資源エネルギー工学部システム工学課長より貴重な意見を頂きましたことに謝意を表します。

記　号

T = temperature 〔℃〕
T_b = bed temperature 〔℃〕
F = feed rate of coal and coal char 〔kg／h〕
U_o = superficial gas velocity 〔m／s〕
U_{mf} = incipient fluidization gas velocity 〔m／s〕
dp = particle diameter 〔mm〕
C_c = Carbon Conversion 〔−〕
C_g = Carbon gasified 〔−〕
H_h = high heating value 〔Kcal／Nm³〕
t = time 〔h〕

文　献

1）平戸，鈴木，二宮：燃料協会誌，62，889（1983）
2）小山，田村，佐藤，有崎：日立論評，66，27（1984）
3）河端，弓山，田崎，本間，武田，千葉，鶴江，鈴木：化学工学協会，第19回秋季大会，SM 303（1985）

Abstract

Oxygen-Steam Gasification of Coal and Coal Char in Fluidized Bed.

Yoneshiro TAZAKI, Shigeo CHIBA, Midori YUMIYAMA
Sengi HONMA, Kunihiro KITANO, Shohei TAKEDA,
Junichi KAWABATA and Satoru SUZUKI

Oxygen and steam are commonly used as the gasification reagents. In general, the reaction temperature increases with the oxygen concentration. Fluidized bed gasifier has the limit of the oxygen concentration because of ash agglomeration.

In this study, the superior limit of the oxygen concentration and compositions of product gas are measured and analyzed.

媒体流動層による食品の凍結

弓山　翠

1. はじめに

冷凍という低温処理法は、食品自体の変質がほとんどなく，復元性が優れていることから，魚，肉，農産物などの素材原料，各種冷凍食品，アイスクリームなどの冷菓に幅広く用いられている。これら冷凍食品の消費量は食生活の合理化にコールドチェーンの充実，発展等も加わり，現在もなお急増中である。なかでも，グリーンピース，小エビ，角切りの人参，馬鈴薯，枝豆などの小さな冷凍食品類は調理も簡便であり，消費量が多い。

一般に食品の凍結に際しては，ある量だけまとめて凍結するブロック凍結が広く行われているが，冷凍時間も長く，少量消費する場合でもブロック全部を解凍しなければならないなど，取り扱いの面でも不便である。

これに対し，バラ凍結は小さな食品をバラの状態で凍結するため凍結時間も短く，凍結後の取り扱いも簡単であることから，次第に多用されてきている凍結方法である。このバラ凍結の１つに流動層凍結方法がある。この方法は，Fig. 1 -(A)に示すように，冷風を吹き上げて食品を流動させながら連続的に凍結するもので[1]，我が国には1971年にスウエーデン製の実用装置が輸入されている[2]。しかし，このように食品の流動化及び冷風から食品への冷熱の移動が，冷風のみによって行われる直接流動層凍結法（Direct Fluidized Bed Freezing，D.F.B.F.）では，グリーンピース程度の大きさの食品を流動させるのに数m／sの冷風の流速が必要であり，動力消費量も大きくなる。

そこで，Fig. 1 -(B)に示すように食品の流動化及び熱移動の仲介物質として，粒径200～1000μmの小さな粒子を流動させた中へ，食品を挿入して凍結する媒体流動層凍結法（Intermediate Fluidized Bed Freezing，I.F.B.F.）が考えられる。この方法については，フランスで研究されている[3]が，粒子の付着などについて検討している報告は見られない。日本でも，粒径７㎜φのポリスチレン球を流動化粒子として100×100×10㎜の魚片を凍結した報告がある[4]が，バラ凍結に関するものではない。

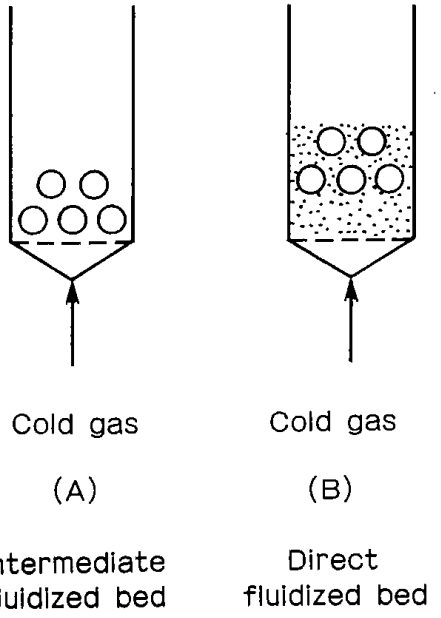

Fig. 1 Contacting modes between cold gas and foods.

また、媒体流動層，直接流動層及び冷凍庫の伝熱特性を比較するためには，それぞれの凍結法における試料の熱伝達率が必要であるが，常温[5,6]や低温[4]状態で測定した報文は少ない。

本報告では，先ず，流動化粒子の流動化性を検討した結果と，黄銅球の冷却実験により熱伝達率を求め，各冷凍法の伝熱特性を比較，検討した結果から食品の流動層凍結の実験条件を設定した。

次に，媒体流動層凍結法により食品の凍結を試み，その凍結速度と品質，流動化粒子の付着，解凍食品の重量減少割合，氷結晶の顕微鏡写真による品質の評価などについて，直接流動層凍結法および冷凍庫凍結法と比較検討した結果について報告する。

2. 実験装置

実験装置は流動層本体，ボルテックスチューブ，コンプレッサーで構成されている。その概略をFig. 2に示す。

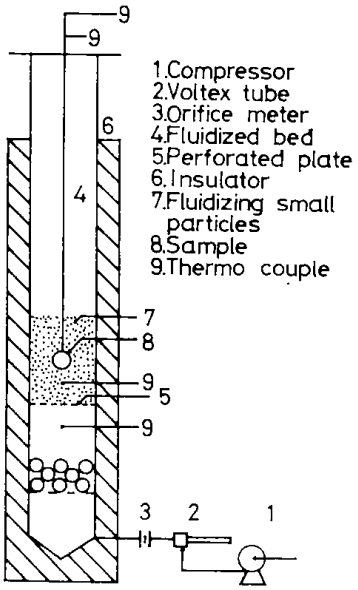

Fig. 2 Schematic diagram of experimental apparatus.

流動層本体は内径75㎜，高さ1000㎜，肉厚5㎜のアクリル製の円筒で，外部から流動状態を観察できるようになっている。流動化空気は，圧縮空気をボルテックスチューブから噴出させ，温度を−40℃〜−50℃に下げ，オリフィスメーターで流量を測定した後，流動層の下部へ吹き込んだ。冷風は，多孔板を通過して流動化粒子を流動させ，同時に流動層を所定の温度に冷却した後，外へ放出した。装置は厚さ50㎜の発泡スチロール板で外側を断熱したが，層内観察のため一部取り外せる構造にした。流動層温度，冷風の流量はボルテックスチューブの開度で調節し，その温度を外径1㎜のシース熱電対（Type-T）で測定した。この装置は冷風のみによって凍結する直接流動層の実験にも使用した。また，冷凍庫凍結には430lit.の大型冷凍庫を使用した。

流動化粒子には，主として，球形に成形したアルミナ粒子を使用した。その平均粒径は520，930 μmの2種類である。他に平均粒径310 μmの精製塩も使用した。

使用した食品は市販されている人参，大根，馬鈴薯で，これらを球形，及び円柱形に切り出して試料とした。その大きさは，外径が0.012，0.018，0.029mの球，及び直径と長さが0.012-0.012，0.018-0.018，0.029-0.029mの円柱である。他にアスパラガス，すだち，小玉葱，芽キャベツも使用した。

伝熱特性を調べるために用いた黄銅球の直径は，0.01，0.02，0.03mである。食品と黄銅球の表面温度及び中心温度は素線径100 μmの熱電対（Type-T）で測定した。

3. 実験条件の検討

3・1 流動化条件

成形アルミナ粒子や大福豆を流動層に充填し，底部から空気を吹き込んで流動させた時の充填物層の圧力損失△Pは，空塔基準のガス流速U_0によってFig. 3のように変化する。

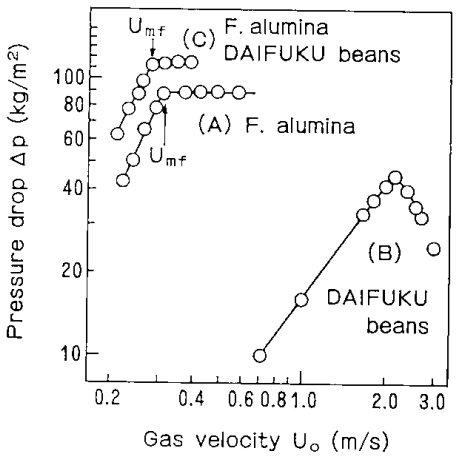

Fig. 3 Relation between pressure drop and gas velocity.

図中の(A)は，平均粒径d_pが520 μmの成形のアルミナ粒子のみを0.45 kg充填した場合で，圧力損失は流速に比例して増加し、ある流速以上で一定

となる。充塡物はこの流速で浮遊状態となり，流動層内に気泡が発生し始める。さらに，これ以上の流速になると，層内に多数の大きな気泡が発生し，混合が激しくなる。この圧力損失が一定になり始める流速が最小流動化速度U_{mf}である。

図中の (B) は大福豆を0.3kg充塡した場合の結果である。大福豆は乾燥したもので，大きさは約0.022×0.014×0.009mで，1個の重さは約1.8gである。この場合は気泡が流動層全体に広がり，大福豆の層がピストンのように押し上げられたり，落下したりするSlugging状態になるため，圧力損失は一定とならず上下に変動する。直接流動層ではこのような流動状態になる可能性が大きい。

図中の (C) は成形アルミナ粒子0.45kgと大福豆0.10kgとを共に充塡した場合である。大福豆はアルミナ粒子や気泡の運動により混合されて良好な流動状態になる。この場合のU_{mf}の値は(A)，(B)の場合よりも小さな値となる[7]。媒体流動層は，このような流動状態である。

また，精製塩とグラニュー糖の流動化性を検討した結果，精製塩の流動状態は良好であり，流動化粒子として充分に使用可能であった。グラニュー糖の場合は，流動化空気が吹き抜けるChannelingの状態となり安定な流動化は困難であった。

3・2 媒体流動層の伝熱特性

媒体流動層中での熱移動は，食品と冷風及び食品と冷却された流動化粒子との間で起こるので，食品の表面における熱移動が凍結速度を左右する。そこで，食品の代わりに黄銅球を用いて熱伝達率を求め，他の凍結法と比較した。

熱伝達率の測定は次のような方法で行った。粒子を流動化させて所定の温度t_bになった流動層内に，瞬間的に直径D_p，温度t_oの黄銅球を挿入，固定し，その中心温度tの変化と時間θの関係を求め，次の熱収支式により熱伝達率h_pを求めた。なお，黄銅球のBi.数は0.032以下と十分小さく，球内部の伝熱抵抗は無視できる。

$$h_p A_p (t-t_b) = -V_p \rho_p c_p \left(\frac{dt}{d\theta} \right) \quad \cdots\cdots\cdots\cdots (1)$$

この式を解いて整理すると次式になる。

$$h_p = \frac{D_p \rho_p c_p}{6} \cdot \frac{\ln((t_o-t_b)/(t-t_b))}{\theta} \quad \cdots\cdots\cdots (2)$$

tとθの関係は，黄銅球を3㎜の黄銅棒の先にネジで取付け，流動層の中心に吊下げて測定した。黄銅球の固定高さHを変えて(2)式により求めたh_pの値をFig. 4に示す。

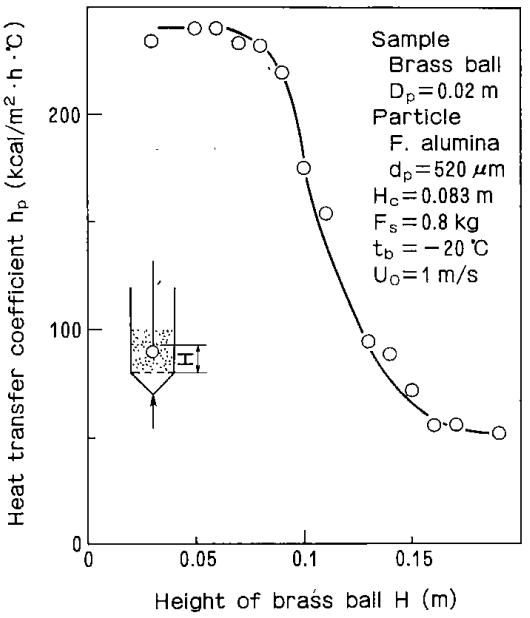

Fig. 4 Vertical distribution of heat transfer coefficient.

h_pは静止層高H_c付近までは大きく，ほぼ一定の値を示すが，これより上部では流動化粒子が希薄になるため急激に減少し，単に冷風のみを吹き付ける強制対流伝熱の値に漸近する。この冷風のみを吹き付ける状態のh_pは直接流動層の場合の値に相当する。この図の結果から，後述する凍結実験では試料を流動層の中心に固定し，その高さをh_pが大きく，ほぼ一定の値を示す0.07mに設定した。

Fig. 5に媒体流動層，直接流動層法及び冷凍庫法によるh_pの値を比較して示した。黄銅球を冷風のみで冷却する直接流動層法のh_pの値は，媒体流動層法の約半分以下であり，冷凍庫におけるh_pの値はさらに小さく5～22kcal/m²•h•℃であった。また，媒体流動層法によるh_pの測定値は，Riosら[5]及び白井ら[6]の値より幾分大きな値を示したが，その差は測定誤差の範囲内にあり妥当な値であると判断できる。

Fig. 6にh_pと（U_o-U_{mf}）の関係を示す。（U_o-U_{mf}）が0.3m/s付近までh_pの値が増加するのは，ガス流速U_oに比例して粒子の運動が激しく

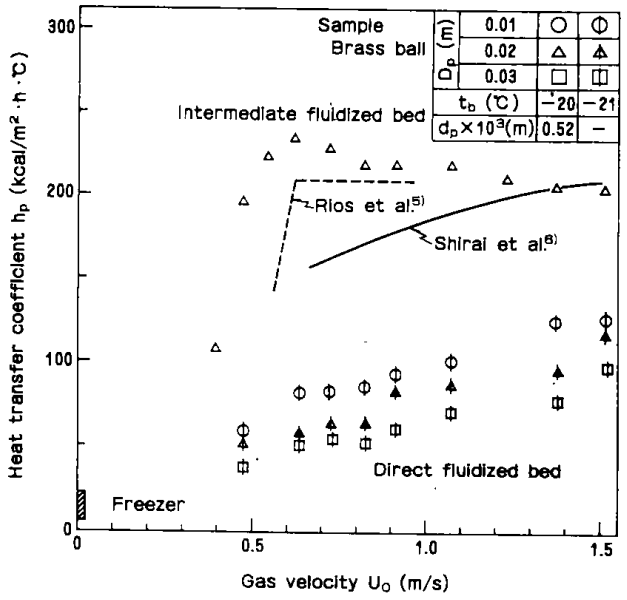

Fig. 5 Relation between gas velocity and heat transfer coefficient in various freezing methods.

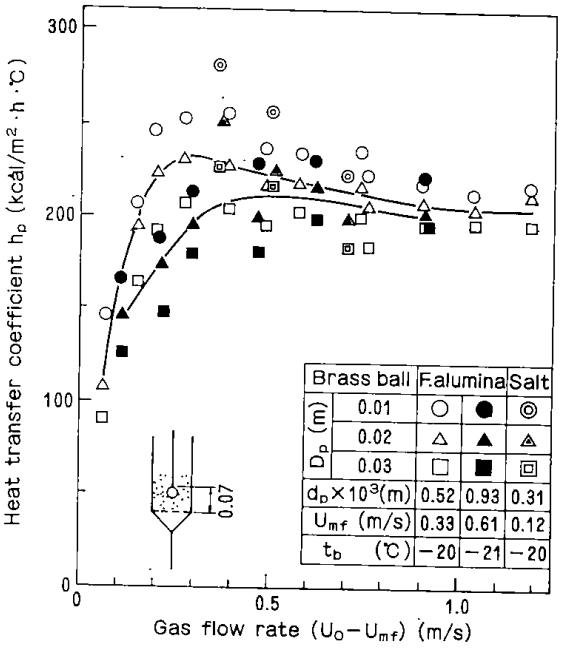

Fig. 6 Relation between gas flow rate and heat transfer coefficient for various size of brass ball. fluidizing particles.

なり，黄銅球に次々と粒子が接触して，個々の粒子が保有する熱の移動が促進されるためである。さらにU_0が大きくなるのに伴いh_pが減少傾向を示すのは，粒子層の密度が粗の状態になり，熱移動量が少なくなったためと考えられる。h_pはd_p及びD_pの小さい方が大きな値を示し，精製塩と成形アルミナとではほとんど同じ傾向と値を示した。

これらの結果から，食品の凍結実験に使用する流動化粒子には，h_pが大きな値を示した520 μ mの成形アルミナ及び精製塩を用い，冷風の流速としては，安定したh_pの値を示す(U_0-U_{mf})＝0.7m／sとすることにした。

4. 食品の凍結実験

4・1 凍結速度

凍結時間と中心温度の変化は，1～2個の食品を黄銅棒の先に針金で挟んで固定してから流動層の中に吊下げて測定した。その測定例をFig. 7に示す。

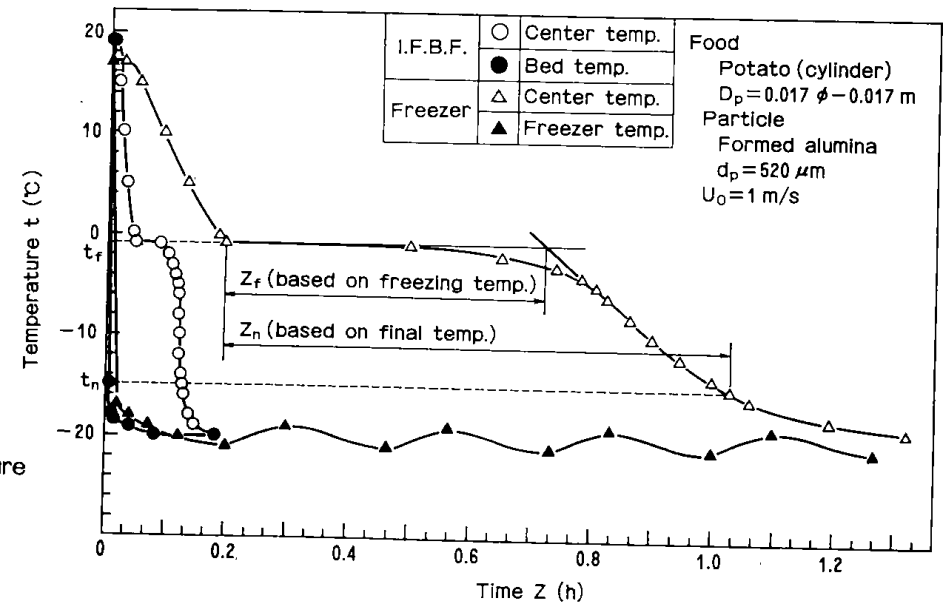

Fig. 7 Relation between time and temperature in various freezing methods.

丸印で示した曲線は媒体流動層，三角印は冷凍庫による凍結の結果である。両曲線とも凍結温度t_fが－1℃付近で，ほとんど一定温度を示すのは，食品中の水分の凍結潜熱によるものである。この温度帯の通過時間が三角印のように長くなると，大きな氷の結晶が生成し，食品の細胞は破られ，解凍時にドリップが流出する原因となる。そのため，以前からこの最大氷結晶生成温度帯の通過時間z_fを小さくするために，冷凍庫内の空気を強制的に循環させたり，食品に液体窒素などを直接吹付けたりする凍結方法が工夫されてきた。

さらに，最近は品質の上から中心部の温度を充分低い温度に冷却することが要求されてきている。I•I•R(International Institute of Refrigeration)では，中心部の最終冷却温度が－15℃以下であることを基準としている。従って，この場合の凍結時間は凍結終温t_nまで冷却するのに要する時間Z_nということになる。

ここで，z_fを凍結時間として$v_f=Dp/2z_f$で求めた凍結速度v_fとD_pの関係をFig. 8に示す。v_fの値によって超急速，急速，中速，緩慢凍結の4段階に区別され[3]，冷凍庫凍結法は，中速凍結に属し，媒体流動層凍結法はD_pが0.029mの場合でも，急速凍結の領域に属している。

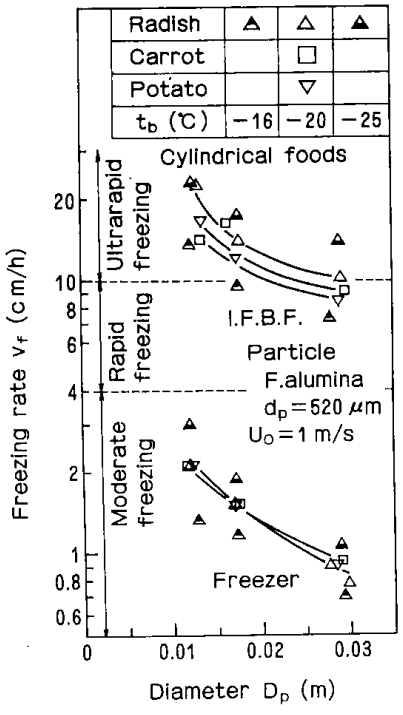

Fig. 8 Relation between food size and freezing rate in various freezing methods.

4・2 熱伝達率

食品の凍結時間を表す考え方の1つは，食品の凍結を水の凍結と同様に考え，凍結層が表面から中心部まで到達するのに要する時間を凍結時間とするものである[8]。

他の1つは，凍結に際し最も温度低下がおくれる食品の中心部の温度が，定められた温度帯を通過するのに要する時間を凍結時間とするものである。

ここで，より実際の凍結を表している後者の考え方に基づいて凍結方程式を解き，球，円柱状食品に対しての凍結時間を求めると次の近似式が得られる[9]。

$$Z_n=\frac{w\gamma\ D_p^2}{4\lambda\ \mu^2}F(t_b,\ t_n) \quad \cdots\cdots (3)$$

$$F(t_b,\ t_n)=c_2\log\frac{(t_f-t_b)}{(t_n-t_b)}-\frac{Lt_f}{t_b}\left(\frac{1}{t_f}-\frac{1}{t_n}\right)$$
$$+\left(c_1-c_2-\frac{L}{t_b}\right)\frac{t_f}{t_b}\log\frac{(t_f-t_b)}{(t_n-t_b)}\cdot\frac{t_n}{t_f} \quad (4)$$

ここで，μ^2の値は次のように表される。
球状食品の場合は，

$$\mu^2=\frac{11.3h_p\ D_p}{(h_p\ D_p+7.4\lambda)} \quad \cdots\cdots (5)$$

円柱状食品の場合は，

$$\mu^2=\frac{6.3\ h_p\ D_p}{(h_p\ D_p+6\lambda)} \quad \cdots\cdots (6)$$

である。(5)(6)式を(3)式に代入し，hpについて整理すると，次式が得られる。
球状食品の場合は，

$$h_p=\frac{7.4\lambda\ w\gamma\ D_p\ F(t_b,\ t_n)}{45.2\lambda\ Z_n-w\gamma D_p^2F(t_b,\ t_n)} \quad \cdots\cdots (7)$$

円柱状食品の場合は

$$h_p=\frac{6\lambda\ w\gamma\ D_p\ F(t_b,\ t_n)}{25.2\lambda\ Z_n-w\gamma D_p^2F(t_b,\ t_n)} \quad \cdots\cdots (8)$$

である。
4・1で述べたようにt_n＝－15℃とすると，Z_n，t_b，t_fは中心温度tの経時変化の測定結果から得られる。また，食品の凍結前後の比熱C_1，C_2，凍結過程における熱伝達率λ，水分w，密度γ，直径D_pは食品によって定まる値であるので，h_pは(7)，(8)式から求めることができる。

C_1, C_2, λ, γなどの値は，食品を水分，脂質，固形分の三成分から成るとして，その水分と脂質から求める式[10]から計算した。水分の値は真空乾燥器で測定した結果，人参が90.6%，馬鈴薯が76.2%であった。一方，日本食品標準成分表[11]によれば人参と馬鈴薯の水分はそれぞれ90.4，79.5%であり，測定値にほとんど等しいことから，他の食品の値もこの成分表の値を用いた。

(3)式の傾向を調べるために，各物性値を代入して求めた計算値と測定値をFig. 9に示した。計算値は凍結温度領域においては良く一致するが，さらに冷却するのに従い，測定値より早い温度降下を示した。この領域の計算値と測定値との温度差は最大で約2℃であり，時間差は最大で約20秒である。

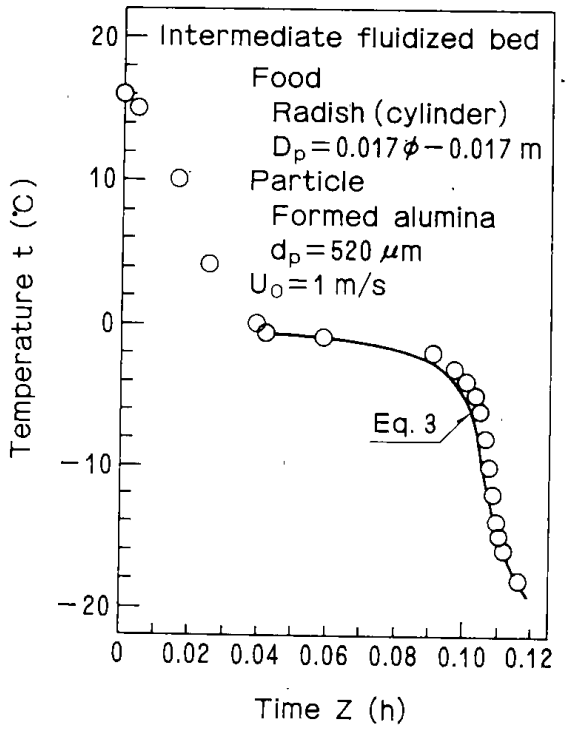

Fig. 9 Comparison between calculated and experimented temperature.

次に，(8)式から求めたh の値をFig. 10に示す。図中の(A)は流動化粒子に成形アルミナを用いた場合であり，(B)は精製塩を用いた場合の結果である。媒体流動層凍結の値は冷凍庫凍結の値より15～20倍大きい。食品の種類によるh_pの値は大根，人参，馬鈴薯の順で小さい値となった。また，h_pはt_bの低い方が大きい値を示し，D_p=0.012mの値は0.029mの約1.5倍の値を示した。(A)と(B)とを

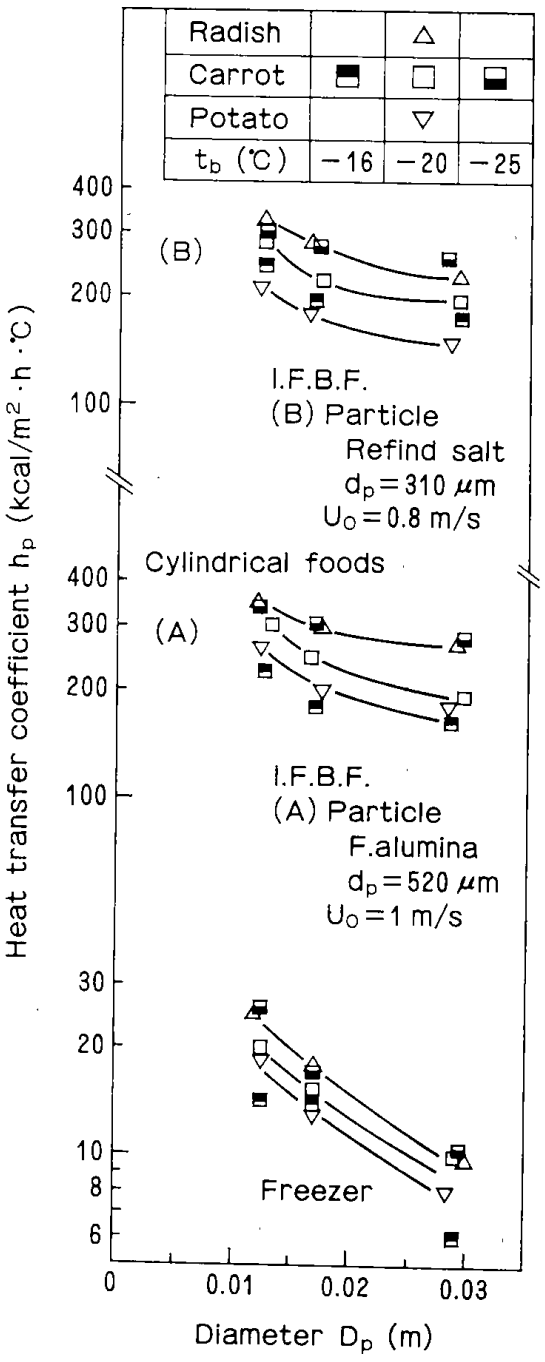

Fig. 10 Relation between food size and heat transfer coefficient for cylindrical foods.

比較すると，h_pの傾向はほぼ同じであるが，その値は精製塩を使用した方が約10%程小さな値を示している。これは凍結する間に食品の表面全体に精製塩が殻のように付着し，熱の移動が抑制されるためである。

球状食品のh_pの測定例をFig.11に示す。媒体流動層凍結の値は，直接流動層凍結の値の約3倍である。球状食品では，D_pが大きくなってもh_pの低下は少ない。小玉葱，すだちなどの皮付き食品のh_pは，切り出した食品の人参，馬鈴薯とほとんど同じ値を示した。芽キャベツが特に小さな値を示すのは，葉と葉の間に形成される空気層によるものと考えられる。

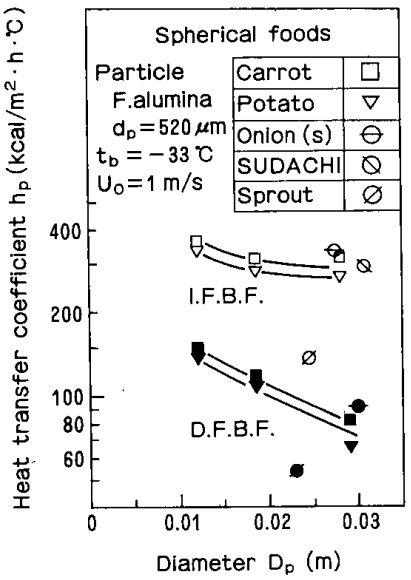

Fig. 11 Relation between food size and heat transfer coefficient for spherical foods.

4・3 流動化粒子の付着

凍結食品への流動化粒子の付着は，媒体流動層凍結においては熱の移動を抑制したり，それ自体が食用物質でなかったりするので，充分留意しなければならない事項である。そこで，成形アルミナを用いた媒体流動層で凍結した食品を，静かに流動層の外へ取り出して自然解凍し，付着した成形アルミナ粒子の重量Mを測定した。なお，精製塩を用いた場合は，解凍の際に付着した塩粒子が溶融するため測定しなかった。

Fig.12に付着量Mの測定結果を示す。図の横軸は流動化粒子が付着可能な食品の表面積A_aである。Mの値は切り出しの際水分が出やすい大根が1番大きく，次いで人参，アスパラガス，馬鈴薯の順になった。食品の形状については，円柱状食品に比較して球状食品の方が著しく小さな値を示した。これは流動化粒子の付着する部位が食品の上部と下部であることから，水平部分の多い円柱状食品の方が付着量も大きくなるためである。また，

小玉葱，すだち，芽キャベツなどは皮付であったり，表面に粘着性がないことから，粒子の付着はなかった。芽キャベツの場合は，葉と葉の間に粒子が挟るため，付着量が大きくなっている。

食品を流動層内に投げ込んで自由に流動させて凍結させた場合（Free）の粒子の付着量は，層内に固定した場合（Fixed）の約⅓であった。図には1個投入した場合の値を示しているが，多数個を入れた場合には，食品と食品の衝突などにより，さらに小さな値が期待できる。

以上の結果から，流動化粒子としては熱伝達率が成形アルミナより約10%小さくなるが，無害物質である精製塩がほとんどの食品の凍結に適当であり，成形アルミナは皮付や粘着性のない食品に適当である。

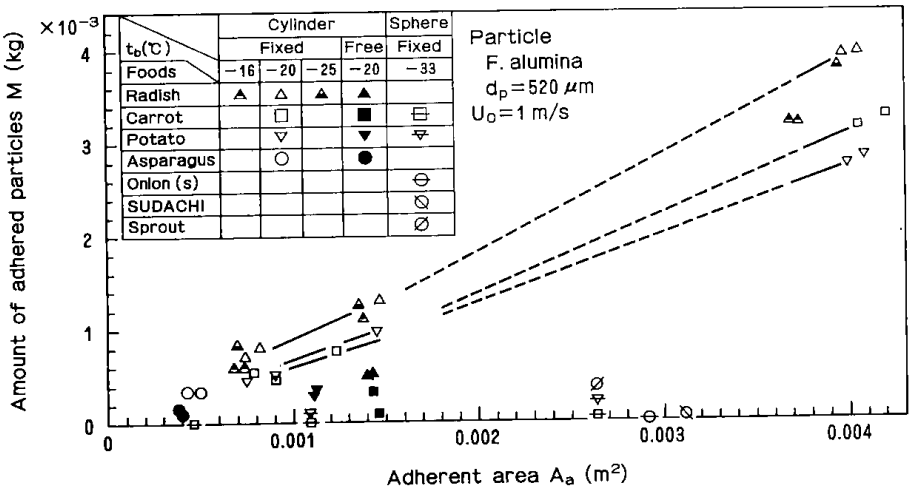

Fig. 12 Relation between adherent area and amount of adhered particles.

4・4　凍結食品の重量減少割合

凍結食品の品質は凍結前と解凍後の食品の重量を測定し，その減少割合で評価した。この値は解凍の方法により異なるが，相対的な値として比較することができ，小さい方が凍結食品の品質としては良好であるといえる。

Fig.13に媒体流動層凍結と冷凍庫凍結とによる重量減少割合YをDp別に示した。Yの値は冷凍庫凍結で最大12%程であるが，成形アルミナを流動化粒子として使用した媒体流動層では最大8%程度と小さな値を示した。食品の種類では馬鈴薯，大根，人参の順で小さな値を示した。また，精製塩を使用した場合は，成形アルミナの場合より大きく，冷凍庫凍結と殆ど同じ値を示した。特に，大根のように表面に水分がにじみ出る食品が最も大きくなり，馬鈴薯，人参の順で小さな値を示した。これは食品の表面の水分が，付着した精製塩によって，より多く浸出したためと考えられる。

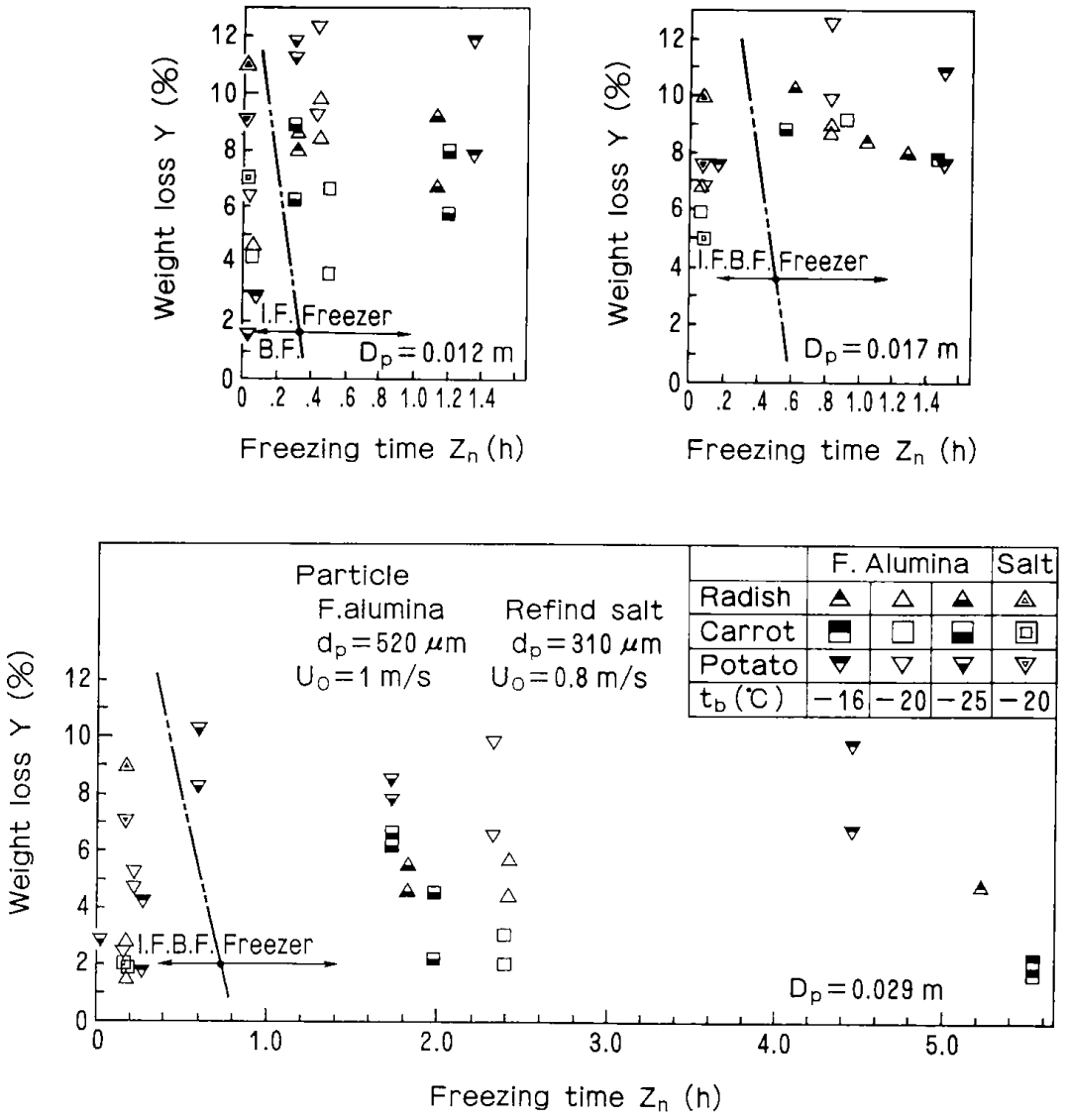

Fig. 13 Relation between freezing time and weight loss.

4・5　氷結晶の顕微鏡観察

凍結食品の品質を判定するもう１つの方法として，顕微鏡写真による氷結晶の観察を行った。Fig. 14にその１例を示す。図中の(A)，(B)に示すように，流動化粒子として成形アルミナ，精製塩を使用した媒体流動層凍結の氷の結晶は丸くて小さく、その大きさも揃っている。これに対し，(C)に示すように，冷凍庫凍結の場合は細長くて大きく，不揃いである。このような氷の結晶の場合には，食品の細胞が破られ，解凍時にドリップが流出するので品質が悪くなる。冷凍庫凍結の場合，氷の結晶が細長いのは，凍結時間が長いため氷の結晶が成長したものと考えられる。

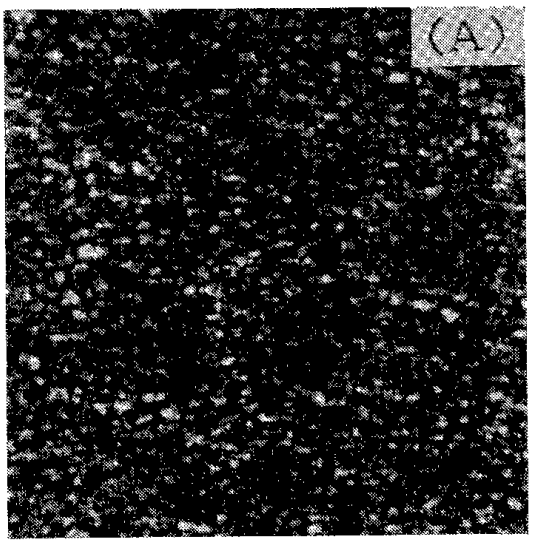

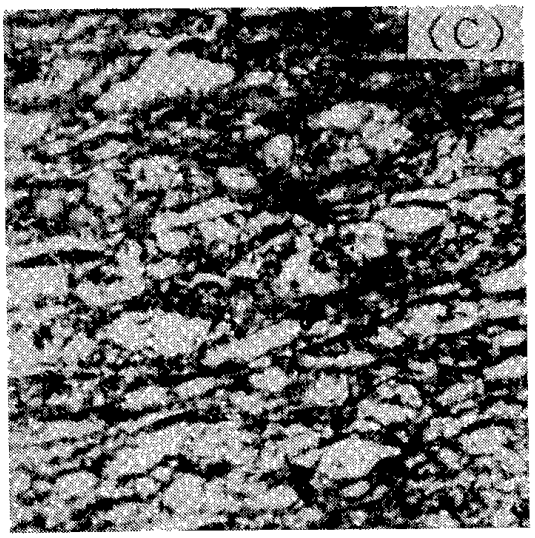

(A)　I.F.B.F.
(Particle : F.alumina, $t_b=-26℃$, $Z_n=0.050h$)

(B)　I.F.B.F.
(Particle : R.salt, $t_b=-27℃$, $Z_n=0.047h$)

(C)　Freezer
($t_b=-27℃$, $Z_n=0.563h$)

Fig. 14　Ice cristals of frozen carrot, 0.017ϕ-0.017m cylinder in various freezing methods.

5. まとめ

媒体流動層，直接流動層，冷凍庫の3種類の凍結法による食品の凍結を行い，以下のような知見が得られた。

(1) 媒体流動層の流動化粒子として使用した成形アルミナ及び精製塩は，流動化性と伝熱特性の両面から適当である。グラニュー糖は流動化性が悪く不適当である。

(2) 媒体流動層凍結の方が直接流動層凍結より吹き込み空気量は少なくて済む。

(3) 媒体流動層，直接流動層，冷凍庫の3種類の凍結方法における熱伝達率の値は，食品の直径が0.02mの場合，それぞれ300，100，15kcal／m・h・℃である。また，精製塩を流動化粒子として使用した場合は，成形アルミナの場合より約10%程小さい。

(4) 凍結温度基準の凍結速度の区分によると，媒体流動層凍結は超急速と急速凍結，直接流動層凍結は急速凍結，冷凍庫凍結は中速凍結の領域に属する。

(5) 球状で，流動層内に固定せず，皮付きの食品の場合，流動化粒子は全く付着しない。また，付着してもその値は小さい。

(6) 解凍食品の重量減少割合は，媒体流動層凍結の方が冷凍庫凍結より小さい。しかし，精製塩を流動化粒子に使用した場合は，成形アルミナの場合より大きい。

(7) 顕微鏡写真の観察によれば，媒体流動層凍結の氷の結晶は冷凍庫凍結より小さく，その大きさも揃っている。

以上の結果から媒体流動層凍結は，直接流動層凍結法，冷凍庫凍結法よりも優れた凍結法である。

謝　辞

本研究を進めるにあたり，貴重な御助言と御協力を戴きました河端淳一材料開発部長，富田稔システム工学課長に深く感謝の意を表します。

記　号

A_a ＝adherent area on food surface　(m^2)
A_p ＝surface area of brass ball　(m^2)
c_1 ＝specific heat of water　(kcal／kg・℃)
c_2 ＝specific heat of ice　(kcal／kg・℃)
c_p ＝specific heat of brass ball　(kcal／kg・℃)
d_p ＝mean diameter of small particle　(μm)
D_p ＝diameter of sample　(m)
F_s ＝weight of small particles　(kg)
h_p ＝heat transfer coefficient　(kcal／m^2・h・℃)
H ＝hight of sample above perforated plate　(m)
H_c ＝static bed height　(m)
L ＝latent heat　(kcal／kg)
M ＝amount of adhered small particle　(kg)
$\triangle P$ ＝pressure drop　(kg／m^2)
t ＝temperature　(℃)
t_b ＝bed temperature　(℃)
t_f ＝freezing temerature of food center　(℃)
t_n ＝final temperature of food center　(℃)
t_o ＝initial temperature of food center　(℃)
U_o ＝superficial gas velocity　(m／s)
U_{mf} ＝minimum fluidization velocity　(m／s)
v_f ＝freezing rate　(cm／h)
V_p ＝volume of sample　(m^3)
w ＝moisture content　(%)
Y ＝weight loss of thawed food　(%)
Z ＝time　(h)
Z_f ＝freezing time based on freezing temperature　(h)
Z_n ＝freezing time based on final temperature　(h)
γ ＝density of frozen food　(kg／m^3)
θ ＝cooling time of brass ball　(h)
λ ＝thermal conductivity　(kcal／m・h・℃)
ρ_D ＝density of sample　(kg／m^3)

引用文献

1) Demichelis, A., Calvelo, A. : J.Food Sci., vol. 50, No.3, p.669 (1985)
2) 加藤舜郎：冷凍空調技術，第22巻，第256号，p.23 (1971)
3) Marin, M., Gibelt, H., Rios, G.M. :

J.of Powder & Bulk Solids Tech., vol.17, No.1, p.21 (1983)
4) 片山功蔵, 斉藤彬夫, 中村文人, 松田謙治: 冷凍, 第56巻, 第641号, p.187 (1981)
5) Rios, G.M., Gibelt, H.: "Fluidization", Ed.by D.Kunii & R.Touei, p.363, Engineering Foundation, 1984
6) 白井 隆, 吉留 浩, 庄司喜彦, 田中重之, 北条公三, 吉田俊二: 化学工学, 第29巻, 第11号, p.880 (1965)
7) 弓山 翠, 平間利昌, 山口 弘: 粉体工学研究会誌, vol.14, No.5, p.3 (1977)
8) Charm, S.F., 細川 明 監訳: "Foundamentals of Food Engineering", p.218, 光琳, 1963
9) 源生一太郎: "現場の食品化学工学", p.177, 化学工業社, 1983
10) 田中和夫, 小嶋秩夫: "食品冷凍工学", p.142, 恒星社厚生閣, 1976
11) 科学技術庁資源調査会: "四訂 日本食品標準成分表", 1982

Abstract

Food Freezing in the Intermediate Fluidized Bed

Midori Yumiyama

A new food freezing method has been investigated using the so-called intermediate fluidized bed in which the food was fluidized togather with small particles for aid of the fluidization and heat transfer of the food.

Formed alumina and refined salt particles for the small particles were fluidized by the air of −40℃ to −50℃ in an acrylnitril resin column of 0.075m I.D., 1 m height and 0.005m thickness. Carrot, radish, potato, onion, asparagus, sudachi and sprout were used for the freezing test samples.

In this freezing method, the heat transfer coefficient showed the large value of about 300 kcal $/m^2 \cdot h \cdot ℃$, the weight loss of frozen food was relatively smaller and the ice crystals in the frozen food were smaller and more uniform, compared with direct fluidized bed and freezer box methods. The adhesion of the small particles on the frozen food was also measured and evaluated.

It was concluded from the experimental results that the food freezing method by the intermediate fluidized bed is superior to those by the direct fluidized bed and the freezer box.

Measurement of ATP content in microbial cell under aerobic and anaerobic conditions

Shigenobu TANAKA, Yuji YOKOTA

Abstract

ATP content in a unit mass of facultative anaerobes growing under aerobic, anaerobic, changing from aerobic to anaerobic and changing from anaerobic to aerobic conditions was measured. Irrespective of conditions, the ATP content showed a similar value in logarithmic growth phase, namely around 2 g ATP • (kg cell)$^{-1}$. This suggests that under anaerobic condition as well as. under aerobic condition ATP measurement can be used to determine the concentration of the viable microbial cells most of which are in the logarithmic growth phase.

Introduction

Determination of microbial cell concentration in a medium is usually carried out by optical methods. When the medium contains suspended matter other than cells, the optical density is affected by the suspended matter. So several alternative indexes of the quantity of viable mass have been proposed including deoxyribonucleic acid (DNA), total protein, Kjeldahl nitrogen, enzyme activity and adenosine triphosphate (ATP). Above all, the measurement of ATP seems to be a useful method for the determination of viable cells in a medium containing suspended matter because ATP is contained only in viable cells and can be determined relatively easily by photometry. Although there are reports[1-3] on the application of ATP measurement to the determination of viable cell under aerobic condition, there is few report on the case under anaerobic condition or changing condition between aerobic and anaerobic ones.

In this paper ATP content of facultative anaerobes which are growing both under aerobic and anaerobic circumstances was measured and its applicability to the determination of cell concentration under anaerobic condition is discussed.

Materials and Method

Microorganism *Escherichia coli* K-10 and a strain[4] belonging to Pseudomonas which has denitrifying activity in nitrate medium under anaerobic condition (this will be named denitrifier hereafter) were used.

Media and culture conditions The composition of the culture medium used is shown in Table 1. The carbon source is glucose (Medium A), citrate (Medium B), and maltose (Medium C).

Table 1. Medium Composition

Component [g • l^{-1}]	Medium A	Medium B	Medium C
$C_6H_{12}O_6$	2.43		
$Na_3C_6H_5O_7 \cdot 2H_2O$		1.7	
$C_{12}H_{22}O_{11} \cdot H_2O$			20.0
Peptone			8.0
$Na_2HPO_4 \cdot 12H_2O$	22.0	22.0	
KH_2PO_4	1.0	1.0	2.0
$MgSO_4 \cdot 7H_2O$	0.05	0.05	
$FeSO_4 \cdot 7H_2O$	0.005	0.005	
KCl	2.8	2.8	0.4
KNO_3	2.0	1.4	

Media A and B were used for denitrifier and Medium C for *E.coli* The experimental apparatus is shown in Fig. 1. Two incubation vessels of 1ℓ volume containing 0.9ℓ of sterilized medium were seeded from agar slant and incubated at 37℃ (310 K). One of the vessel was used for aerobic incubation where 2.39mℓ• s^{-1} of air was aerated through a cotton filter. The other vessel was used for anaerobic incubation where the medium was sealed by about 10㎜ thick liquid paraffine. In the case of changing condition from aerobic to anaerobic or from anaerobic to aerobic, nitrogen gas instead of air was blown through the medium during anaerobic condition. Both of the vessels were continuously stirred by a magnetic stirrer keeping the cells in a suspended state. The rubber stopper of the vessel was equipped with a sampling tap and from this tap about 4 mℓ of the medium was sampled with a syringe at predetermined intervals.

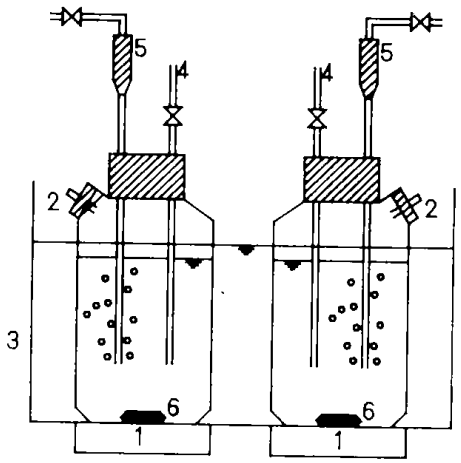

1 Magnetic stirrer
2 Exhaust pipe
3 Thermostatic bath
4 Sampling tap
5 Cotton filter
6 Stirrer bar

Fig. 1 Experimental apparatus

ATP Assay One milliliter of the sample was added to 9 mℓ of Tris buffer solution (0.02M, pH 7.75) and ATP was extracted by boiling the mixture for 10 minutes. An integrating photometer, model 2000 from SAI Technology Co., was used to assay ATP by the luciferin-luciferase reaction. The reaction mixture consisted of 0.5 mℓ extracted sample and 0.5 mℓ reconstructed firefly lantern extract Sigma FLE-50. After 15 seconds of preperation of reaction mixture, the light intensity was integrated for 60 seconds. Calibration curve was prepared using SAI ATP.

Measurement of cell concentration The cell concentration was obtained from optical density at 660 nm.

Effects of the circumstances (aerobic or anaerobic) and of the change in circumstance (from aerobic to anaerobic or from anaerobic to aerobic) on the ATP content in the cell were examined.

Results and Discussion

The measured ATP, cell concentration and calculated ATP content in the cell are shown in Figs. 2~6.

Figure 2 shows the result for *E.coli.* growing in Medium C under aerobic and anaerobic conditions. Figures 3 and 4 show the results for the denitrifier growing in Media A and B, respectively. Figure 5 shows the result for the denitrifer growing in Medium A for the case where in the course of anaerobic logarithmic growth phase the condition was changed to aerobic one. Figure 6 shows the result for the denitrifier growing in Medium A for the case where in the course of aerobic logarithmic growth phase the condition was changed to anaerobic one. In the range of low cell concentration, as it is difficult to determine the cell concentration, ATP content showed some scattering.

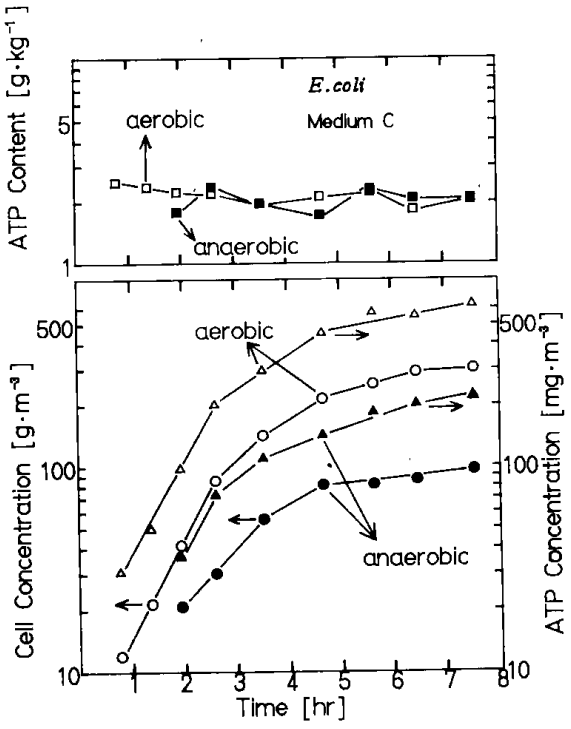

Fig. 2 Time course of ATP content for *E.coli*

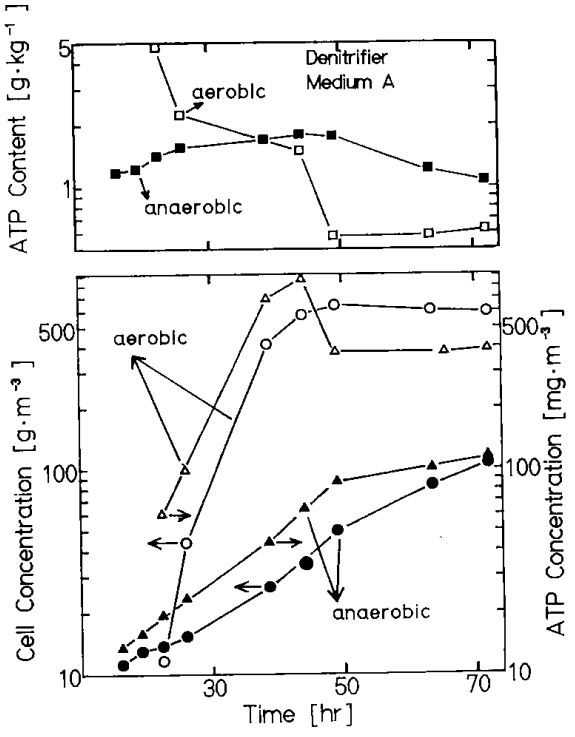

Fig. 3 Time course of ATP content for denitrifier

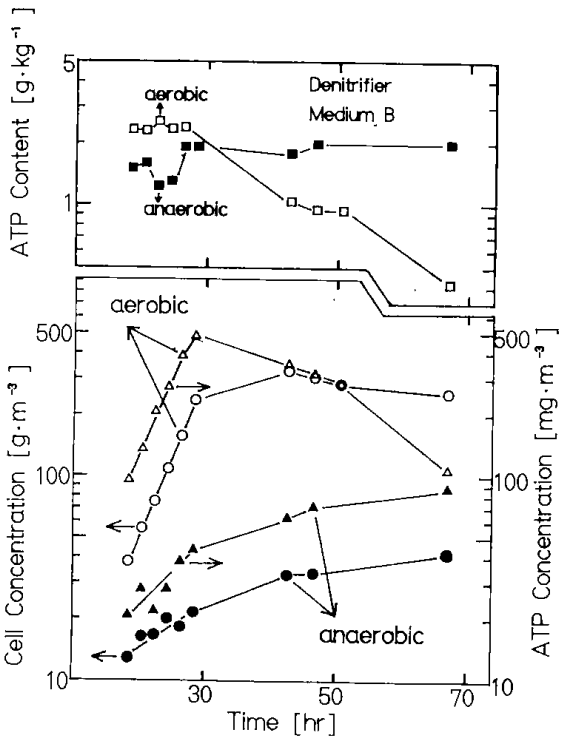

Fig. 4 Time course of ATP content for denitrifier

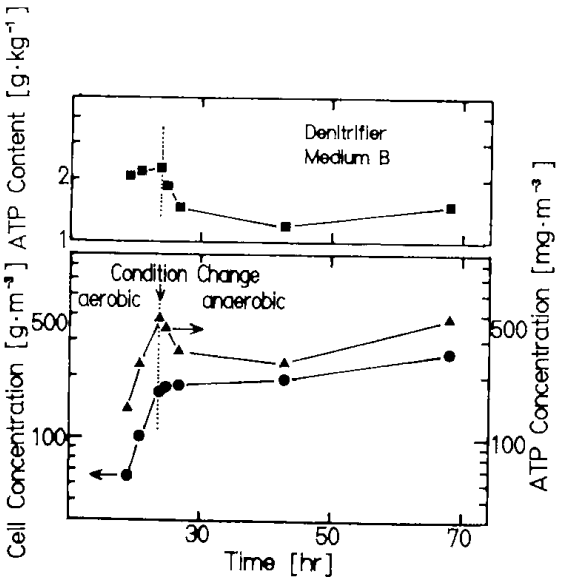

Fig. 5 Time course of ATP content for denitrifier under changing condition

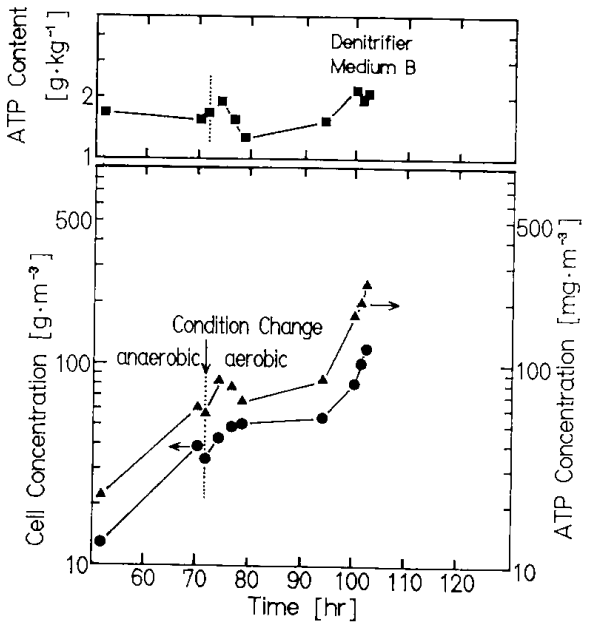

Fig. 6 Time course of ATP content for denitrifier under changing condition

From these results following information was obtained.

1) In the logarithmic growth phase, ATP increases in proportion to the increase in cell concentration under anaerobic condition as well as under aerobic condition. In the stationary phase, ATP decreases more than cell concentration does, therefore ATP content in a unit mass of cell decreases.

2) Although the logarithmic growth rate under anaerobic condition is smaller than that under aerobic condition, ATP content in a unit mass of cell is similar in both cases, namely around 2g ATP• (kg cell)$^{-1}$.

3) When the condition is changed from aerobic to anaerobic or from anaerobic to aerobic in the course of logarithmic growth phase, the organism stops to grow for a long period for either case. Afer that period it starts to grow again and ATP content in a unit mass of cell in the latter growth period is almost the same as that in the former growth period.

These information suggests that under anaerobic condition as well as under aerobic condition ATP measurement can be used to determine the concentration of the viable microbial cell most of which are in the logarithmic growth phase.

Acknowledgements

The authors thank Mr.K. Ishizaki and Dr.H.Matsuyama for providing *E.coli* and the denitrifier, respectively.

Literature Cited

1) Brezonic, P.L. and J.W.Patterson : *J. San. Eng., Div., Amer. Soc. Civil Eng.,* 97, 813 (1971)

2) Hendy, N.A., and Gray : *Biotechnol. Bioeng.,* 21, 153 (1979)

3) Hysert, D.W., F.B. Knudsen, N.M.Morrison and G.van Gheluwe : *ibid,* 21, 1301 (1979)

4) Matsuyama, H. and K.Ishizaki : *Japan Journal of Water Pollution Research,* 5, 161, (1982)

Production of Slow-Release Type Fertilizer from Philippine Dolomitic Limestone and Rice Husks

Katsutoshi Yamada*, Toshio Ogata*, Yoshio Noda *,
Koichi Nakagawa *, Kensaku Haraguchi , Katsuji Ishibashi*,
Alberto R. Caballero**, Marilyn T. Usita**,
Lourdes A. Manalo**, Corazon G. Magpantay**,
Medelyn A. Manalo**, Ofelia G. Atienza **,
Violeta P. Arida**

* : Government Industrial Development Laboratory, Hokkaido
** : Industrial Technology Development Institute (Philippines)

Summary

Production of Slow-Release Type Fertilizer from Philippine Dolomitic Limestone and Rice Husks

Using Philippine dolomitic limestone and rice husks, production tests of a silicate salt matter fertilizer which contained acid-soluble K_2O were carried out. K_2CO_3 reagent was used for potassium additives. Dolomitic limestone and rice husks were mixed with 4.9—20.3% K_2CO_3, and the powder mixture were heated 700—900℃ in air. The roasted products were analyzed, and the amounts of 0.5N HCl-soluble SiO_2, CaO MgO and 2% citric acid-soluble K_2O were determined.

From the experiments the following results were obtained :

1) Under similar conditions of time, the formation of 0.5N HCl-soluble SiO_2 seemes to require a higher temperature.
2) The optimum mole ratio of $(CaO+MgO+K_2O)/SiO_2$ was found to be 2.0 to 2.5 for the fertilizer.
3) The addition of a suitable amount of K_2O was favorable for the increase of 0.5N HCl -soluble SiO_2.
4) The effect of reaction time showed that reactions conducted for 30 minutes produced the same results for 0.5N HCl-soluble SiO_2 as those carried for longer periods of time.
5) Similarly, higher concentration of K_2O in the material mixture enhanced the formation of more 0.5N HCl-soluble SiO_2 in the roasted products.
6) 0.5N HCl-soluble SiO_2 compoment obtained was about 22%, and the 2 % citric acid-soluble K_2O was about 16% in the roasted products.

INTRODUCTION

This research project aims to produce slow-release type fertilizer using philippine dolomitic limestone and rice husks as starting materials.

The philippines is endowed with natural resources of dolomitic limestone reaching about 260 million tons, as of 1983. It is mainly used as soil conditioner, although it also finds application in the manufacture of glass, iron and steel, refractory, as building materials for dolomite plaster, as road ballast and scrubber among others. To the present, it remains a low value material.

Philippine production of rice reached about 8.2 million tons in 1984, producing 1.6 million metric tons of waste rice husks. Although about half of this bulk is utilized as fuel, animal feed and poultry livestock beddings, the remaining half is just burned in the field and wasted, the disposal of which remains a major problem.

The demand for fertilizers in agricultural countries particularly of the developing countries such as the philippines, has in recent years been on the increasingly upward trend side by side with the increased need to maximize production of crops particularly rice. To fill this great demand, the production of fertilizers has been increased in many parts of the world. Studies are also being conducted with the end in view of improving the efficiency of fertilizers. Recent fertilizer technology reveals the advent of the slow-release type of fertilizer which has the unique characteristics of controlled nutrient release such that single fertilizer application results in sustained fertilizetion without danger of plasmolysis or fertilizer burns. The obvious advantages of this type of fertilizer includes savings on labor, reduced possibility of fertilizer burns and reduction in element losses through slow-release at a rate corresponding very nearly to the needs of the crop.

CHARACTERIZATION OF RAW MATERIALS

The first phase of the research project included the determination of the physical and chemical properties of dolomitic limestone and rice husks materials to be used in the experiments. Characterization of these materials was carried out to determine the properties which could make them suitable for the production of slow-release silicate fertilizers.

This chapter presents the results of analysis made on these materials, using various methods and the conclusions derived therefrom.

1. RAW MATERIALS

1・1 Dolomitic Limestone

Philippine dolomitic limestone is a non-metallic mineral containing 97.7% dolomite, a double carbonate of calcium and magnesium, $CaMg(CO_3)_2$ and 2.3% calcite, $CaCO_3$. It

is a commodity which at present finds application in the manufacture of brick mortars, glass, paper, refractories, iron and steel among others. The dolomitic limestone used in the study was obtained from the Philippine Mining Service Corporation, Cebu, Philippines.

1・2 Rice Husks

Rice husk are cellulosic fibrous, non-digestible by product material obtained from the milling of paddy rice and are an agro-waste. Unmilled rice yields about 20% by weight of rice husks, which on combustion loss behind about 25% of ash composed essentially of silica. This silica is originally present in the cellulose lignin woody matter in the form of hydrated opaline phase. Rice husks and rice husks ash obtained from various parts of the Philippines were used in the study.

1・2・1 Raw Rice Husks

Raw rice husks used in the study were of the IR 54 variety obtained from rice mill in Laguna, philippines.

1・2・2 Rice Husks Ash Generated from the Thermal Power Plant of the National Food Authority

Rice husks ash was also procured from the rice husks fed thermal power of National Food Authority (NFA), in Cabanatuan City, Nueva Vizcaya, Philippines.

Rice husks have heating valu of 12.5—15.9 MJ/kg and are cheap and renewable source of energy. In the NFA thermal power plant, rice husks are used to generate steam to produce 315kw of electricity which in turn are used to run rice mill in the area. Intermittent operation of the power plant produces a substantial amount of rice husks ash.

Random samples of the generated waste rice husks ash were obtained at various spots in the furnace and mixed thoroughly for use in the study.

2. ANALYSES

2・1 Chemical Analysis

The chemical composition of philippine dolomitic limestone and rice husks were each determined by inductively coupled plasma (ICP) analysis, using the Shimazu Inductively Coupled Plasma Emission Spectrometer GVM-1000P with a linear flow nebulizer.

The ignition loss of dolomitic limestone and rice husks were also determined by the Japanese Industrial Standard (JIS) methods using a muffle furnace at 925℃.

2・2 Thermal Analysis

The thermal decomposition of dolomitic limestone and rice husks were determined from both thermogravimetric (TG) and differential thermal analysis (DTA) by Rigaku Thermoflex Model 8112-RH using α-Al_2O_3 as the reference sample. The TG curve shows the loss in weight of the sample with respect to changes in temperature ; the DTA curve on the other hand, illustrates the temperature difference between the sample and the reference standard with respect to changes in temperature or time. It shows the temperature at which the decomposition of a sample takes place.

Thermal analysis of dolomitic limestone was carried out both in air and in CO_2 atmospheres. For rice husks, only air atmosphere was used. Heating rate was 20℃/min ; CO_2 flow rate, 80 mℓ/min.

Comparative analysis were also undertaken on the thermal decomposition of a mixture of dolomitic limestone and rice husks ash and an admixture of the two with potassium carbonate. The addition of the latter, K_2CO_3, was aimed at studying its effect on the

decomposition temperature of dolomitic limestone. Heating rate used was 20℃/min under air atmosphere.

2・3 X-ray Diffraction Analysis

Dolomitic limestone, rice husks and rice husks ash were each subjected to X-ray diffraction analysis using a Rigaku X-ray Diffractometer Mode HV-21. The X-ray beam source was a copper tube with a nickel filter.

2・4 Surface Area Analysis

Internal surface area determination was measured by nitrogen gas adsorption apparatus, using Quantasorb Mobel OS-8. This involves the B.E.T. method of adsorption which is the adsorption of nitrogen gas at −196℃.

2・5 Scanning Electron Microscope

The microstructure was observed through a JEOL Scanning Electron Microscope Model JSM-TSO using an acceleration voltage of 20kv. Rice husks were prepared by ashing the sample in a furnace for one hour at 850℃ and coated with gold ion by means of a vacuum evaporator.

2・6 Proximate Analysis

Proximate analysis of rice husks ash used in the study was determined from thermogravimetric analysis. Comparative analysas were carried out for NFA rice husks ash.

3. RESULTS AND DISCUSSIONS

3・1 Chemical Analysis

Table 1 summarizes the chemical composition of philippine dolomitic limestone and rice husks as determined by ICP analysis. The table shows that dolomitic limestone contains mostly CaO and MgO with traces of other components. CaO/MgO ratio was 1.72.

Table 1. Chemical Composition of Philippine Dolomitic Limstone and Rice Husks

Constituents	Dolomitic Limestone (%)	Rice Husks (%)
SiO_2	0.35	24.78
CaO	34.46	0.08
MgO	20.09	0.07
Al_2O_3	0.65	—
Fe_2O_3	0.12	0.10
K_2O	0.02	0.11
Na_2O	0.04	0.06
TiO_2	0.01	—
Loss on ignition	44.26	74.80

* : all constituents expressed as oxides

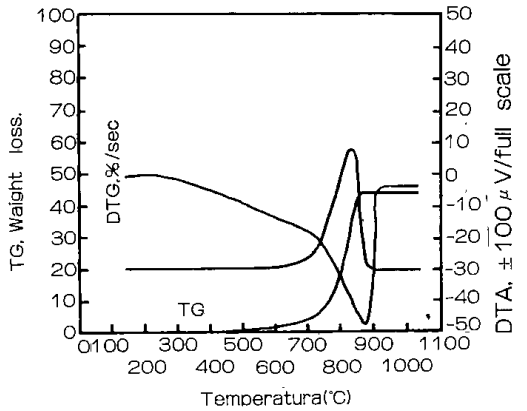

Fig.1 Thermal analysis of Philippine dolomitic limestone
Ref. sample : α-Al2O3
Program rate : 20℃/min.
Atmosphere : air

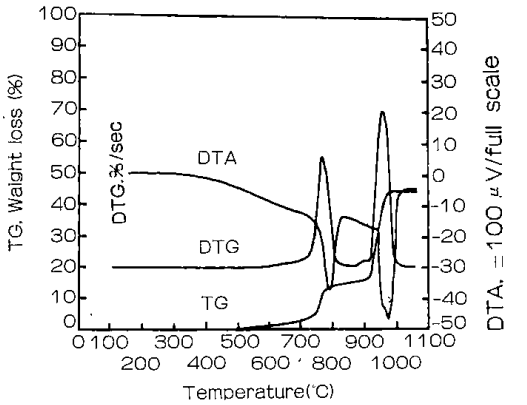

Fig. 2. Thermal analysis of Philippine dolomitic limestone
Ref. sample : α- Al2O3
Program rate : 20°C/min
Atmosphere : CO2, 80ml/min.

3 • 2 Thermal Analysis

3 • 2 • 1 Dolomitic Limestone

Figures 1 and 2 show the thermal decomposition curve of Philippine dolomitic limestone as observed under air and CO_2 atmospheres respectively. As shown by the DTA curves, the decomposition of dolomitic limestone is an endothermic reaction, which under air atmosphere is observed to be a single step reaction. The decomposition of $CaCO_3$ and $MgCO_3$ in the dolomite exists simultaneously at 875℃. Under CO_2 atmosphere, however, the decomposition of these components occur at different temperatures, as shown by the two DTA peaks. $MgCO_3$ decomposes faster at 770℃ while $CaCO_3$ decomposes at 975℃. The observation is likewise shown in the DTG curve. The decomposition reactions are summarized as follows :

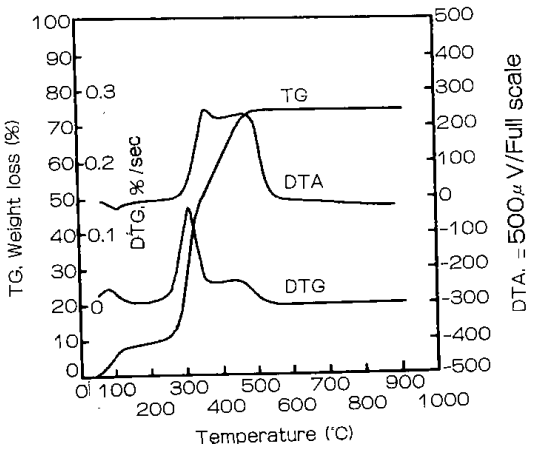

Fig. 3. Thermal analysis of Philippine rice husks
Ref. sample : α - Al2O3
Program rate : 20℃/min.
Atmosphere : air

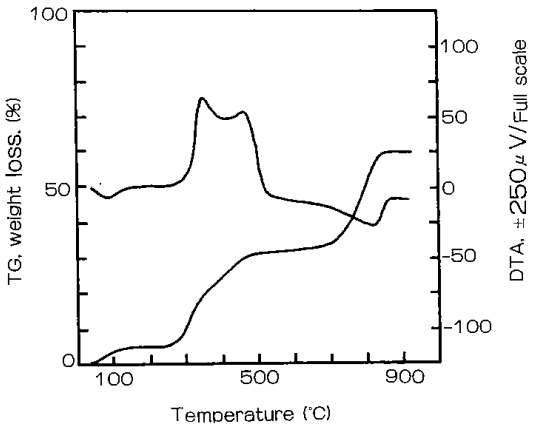

Fig. 4. Thermal analysis of a mixture of dolomitic limestone and rice husks
Ref. sample : α - Al2O3
Program rate : 20°C/min.
Atmosphere : air

Under air atmosphere :

$CaMg\ (CO_3)_2 \rightarrow MgO + CaO + 2CO_2 (T = 875℃)$

Under CO_2 atmosphere :

$CaMg\ (CO_3)_2 \rightarrow MgO + CaCO_3 + CO_2 (T = 770℃)$

$CaCO_3 \rightarrow CaO + CO_2 \quad (T = 975℃)$

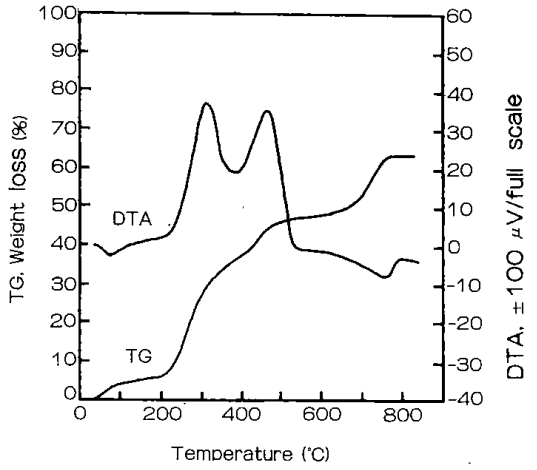

Fig. 5. Thermal analysis of a mixture of dolomitic limestone, rice husks and K_2CO_3
Ref. sample : α - Al_2O_3
Atmosphere : air

3・2・2 Rice Husks

Figure 3 shows the thermal decomposition of raw rice husks under air atmosphere. From the DTA curve it is seen that this reaction is an exothermic decomposition reaction. The DTG curve on the other hand, shows 3 peaks corresponding to the evolution of moisture at 120℃, volatile combustible matter at 200−340℃ and the degradation of cellulosic matter at 304−520℃.

Figure 4 shows the thermal decomposition of a mixture of 38.7% rice husks ash and 61.3% dolomitic limestone. It was observed that while the decomposition reaction of dolomitic limestone occurs at 875℃, the mixture of rice husks and dolomitic limestone decomposes at lower temperature, as shown by the DTA peak as 816℃. With the addition of K_2CO_3 decomposition of the mixture occurs even at a lower temperature of 754℃ as shown in Figure 5. Decomposition starts at 600℃ and finishes at 775℃ respectively. Thus, the presence of K_2CO_3 not only lowers the decomposition temperature of the mixture but also shortens the duration of the decomposition reaction.

3・3 X-Ray Diffraction Analysis

Figure 6 illustrate the X-ray diffraction pattern of Philippine dolomitic limestone and shows X-ray peaks corresponding to dolomite, $CaMg\ (CO_3)_2$ and calcite, $CaCO_3$. Although it consists mainly of dolomite, it also contains small quantities of calcite which gives it the properties of a limestone.

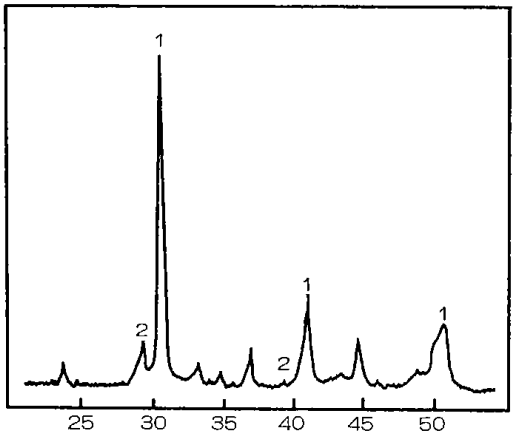

Fig. 6 X-ray diffraction pattern of Philippine dolomitic limestone

1 : $CaMg(CO_3)_2$, 2 : $CaCO_3$

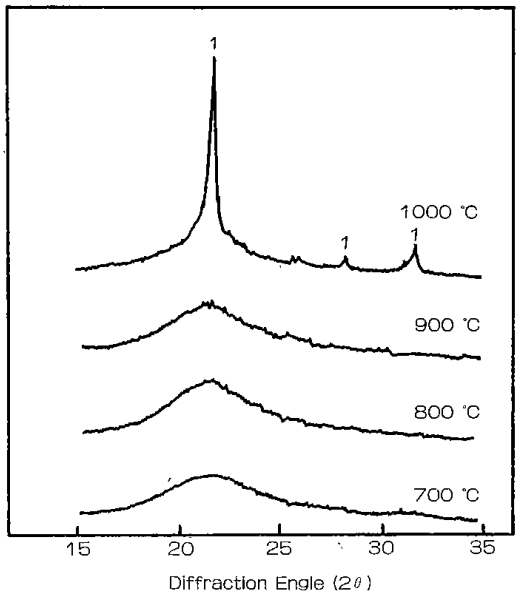

Fig. 7. X-ray diffraction pattern of rice husks ash obtained at various temperatures. at reaction time of 10 minutes

1 . Cristobalite

Figure 7 illustrates the X-Ray diffraction pattern of rice husks ash obtained after heating rice husks at various temperatures for 10 minutes. At temperatures between 700—900℃, the ash is observed to be amorphous. However as the temperature is increased to 1000℃, the silica transforms to a crystalline form witn the formation of a cristobalite phase ; which compared to amorphous silica, is more difficult to react. The order of increasing ease of reactivity of silica is as follows :

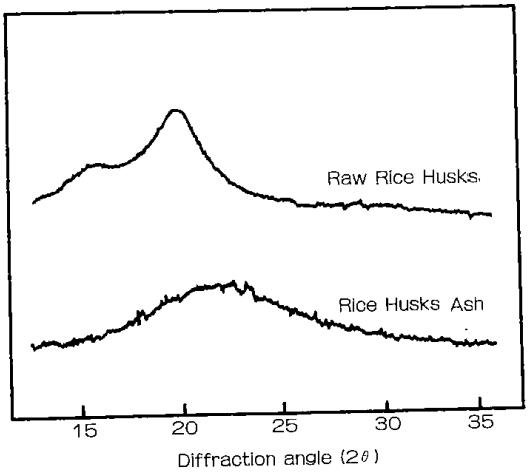

Fig. 9. X-ray diffraction parttern of Philippine rice susks and rice husks ash

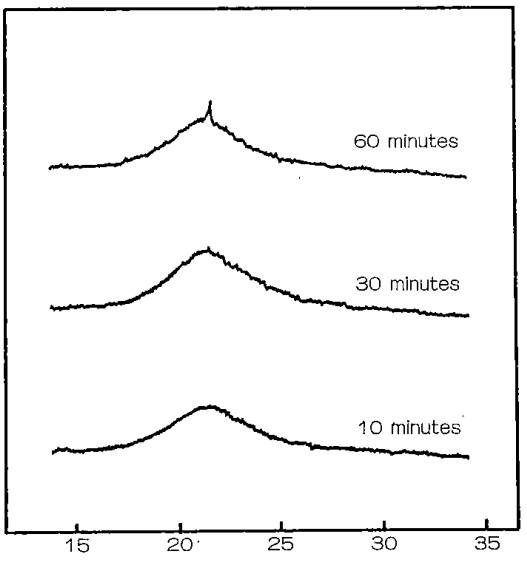

Fig. 8. X-ray diffraction pattern of Philippine rice husks ash produced at varying reaction time at 900 ℃

amorphous silica > cristobalite > tridymite > α -quartz

Even at a temperature of 900℃, the slight transformation to crystalline silica is also observed when the heating time is prolonged to 60 minutes as shown in Figure 8.

The X-ray pattern of rice husks ash obtained from the NFA thermal power plant revealed the presence of amorphous silica as shown in Figure 9.

Combustion of these rice husks containing amorphous silica was carried out at temperatures below 900℃.

Fig. 10. Surface of the rice husks ash in the Scanning Electron Microscope (SEM)

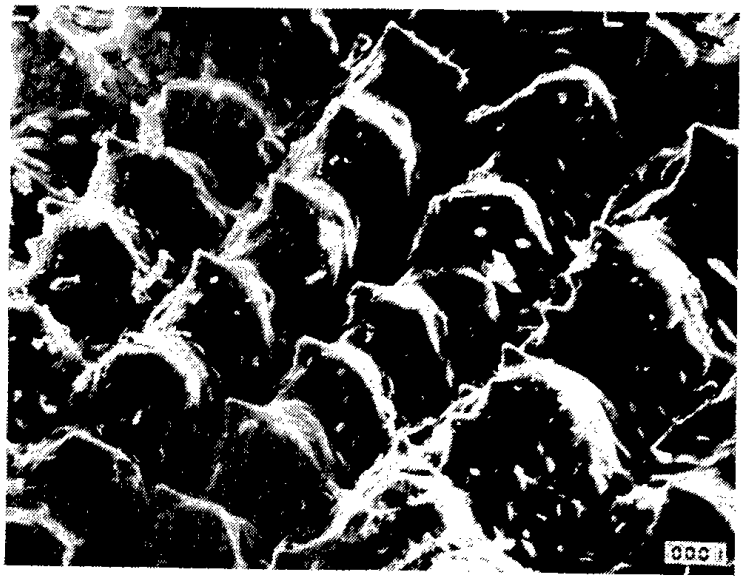

a) : Magnification; X 500 L 100μm L

b) : Magnification; X 1500 L 10μm L

3・4 Surface Area Analysis

Amorphous rice husks ash obtained at firing temperature of 900℃ gave a high surface area of 40㎡/g. This result fortifies the fact that the rice husks ash is reactive.

3・5 Scanning Electron Microscopy

Figure 10 illustrates the microstructure of rice husks ash prepared at 900℃ as defined by scanning electron microscope. The micrograph of the ash reveals a multilayered cellular structure which has remained undamaged by heating at high temperatures.

3・6 Proximate Analysis

Table 2 summarizes the comparative proximate analysis of the NFA rice husks ash. The NFA ash which is generated by the rice husks fed thermal power plant is shown to contain a higher percentage of fixed carbon.

Table 2. Results of the Proximate Analysis of Rice Husks Ash by Thermogravimetry

	Moisture (%)	Ash (%)	Residual Carbon (%)
NFA Rice Husks Ash*	12.00	69.50	18.70

* : Ash obtained from the NFA thermal power Plant in Cabanatuan

4. CONCLUSION

Characterization of the raw materials to be used in the study have been carried out. Philippine dolomitic limestone and rice husks either alone or in combination with each other revealed the following interesting reaults :

1. Philippine dolomitic limestone is a mixture of 97.7% dolomite and 2.3% calcite as revealed by chemical composition data. It contains 34.46% CaO and 20.09% MgO.
2. Rice husks contains reactive amorphous silica which remains unchanged after heating to 900℃ for less than 1 hour ; on heating at 1000℃, the silica transforms to cristobalite which in comparison with amorphous silica is more difficult to react. Rice husks ash exhibits a surface area of 40㎡/g.
3. Thermal decomposition of dolomitic limestone into CaO and MgO occur at 875℃ under air atmosphere ; in combination with rice husks, it decomposes at 816℃ ; with the addition of K_2CO_3 to this mixture, decomposition temperature drops to a much lower temperature of its decomposition temperature for 853℃ to 754℃ and this temperature facilitates the on-set of the reaction.

BASIC STUDIES ON THE PRODUCTION OF SLOW-RELEASE TYPE FERTILIZER

The second phase of the study involved the establishment of the reaction parameters required in the production of the slow-release type fertilizers from dolomitic limestone and rice husks. Basic heat treatment studies were carried out on various mixtures of dolomitic limestone and rice husks in a muffle furnace at varying conditions of temperature, time, reactant mole ratio and concentration of the auxiliary material K_2O. The effect of these parameters was evaluated on the basis of the solubility and hence, availability of silicon, calcium, magnesium and potassium in the heat treatment products as measured by their solubility in 0.5N HCl, 2% citric acid and water.

Preliminary heat treatment experiment was first conducted on a mixture of rice husks and dolomitic limestone. Comparative run was also carried out on a sample mixture of these two materials with the addition of potassium containing material such as K_2CO_3. Based on these findings in the initial study, more intensive experiments were carried out which were geared towards finding the best conditions required to produce the desired silicate fertilizers. The ultimate objective in these experiments was to obtain a fertilizer product which has the properties approximating those of the specified standard fertilizers, namely a high content of acid-soluble SiO_2 and low content of water-soluble K_2O among others.

This chapter describes the experimental work conducted in these basic studies and the results derived from the series of experiments. Comparative studies are reported on the use of raw rice husks and rice husks ash as sources of silica.

1. PREPARATION OF RAW MATERIALS

1・1 Preliminary Experiments

Dolomitic limestone and rice husks were first pulverized separately to pass a 200 mesh sieve. A sample mixture coded as Sample 1 was prepared containing 61% dolomitic limestone and 39% rice husks based on sample weight. Another sample was prepared which contained 30% dolomitic limestone, 50% rice husks and 20% K_2CO_3 as source of potassium. This was labelled as sample 2. The K_2CO_3 solution was slowly added to the mixture of dolomitic limestone and rice husks and mixed thoroughly. The sample mixture was then dried at 110℃ for 2 hours and pulverized to pass a 200 mesh sieve.

1・2 Experiments using Rice Husks

A series of sample mixtures of dolomitic limetone and rice husks were prepared in varying proportions witn the addition of potassium carbonate as the source of potassium. Samples containing varying mole ratios of $(CaO+MgO+K_2O)/SiO_2$, 1, 2, 2.5 and 3, were prepared. The mole ratio was colculated based on the known concentration of CaO and MgO in the dolomitic limestone, SiO_2 in rice husks and K_2O in K_2CO_3 as determined previously. Table 3 shows the proportionate amounts of dolomitic limestone, raw rice husks and K_2CO_3 used for the different samples.

Table 3 . Proportionate Amount of Raw Rice Husks, Dolomitic Limestone and K_2CO_3 in the Sample Mixtures

Sample No.	Rice Husks (g)	Dolomitic Limestone (g)	K_2CO_3 (g)	K_2O (%)	Mole Ratio*
1 − 1	140	54.9	5.1	5.1	1
1 − 2	140	48.8	10.2	10.2	1
1 − 3	140	36.4	20.4	20.3	1
2 − 1	170	121.5	8.5	5.1	2
2 − 2	170	113.0	17.0	10.1	2
2 − 3	165	101.0	34.0	19.5	2
3 − 1	155	136.3	8.7	5.0	2.5
3 − 2	153	129.6	17.4	9.8	2.5
3 − 3	156	113.2	36.8	19.4	2.5
4 − 1	140	151.0	9.0	5.0	3
4 − 2	140	142.0	18.0	9.9	3
4 − 3	135	127.0	38.0	20.1	3

* $(CaO+MgO+K_2O)/SiO_2$ mole ratio

Dolomitic limestone and rice husks were first pulverized separately in a ball mill to pass a 200 mesh sieve ; raw rice husks were pre-heated to 140℃ to facilitate pulverization. The pulverized samples were then dissolved in a solution of K_2CO_3 in a 1-liter beaker and the solution mixed thoroughly using a magnetic stirrer for about 20 minutes. The homogeneous mixture was then transferred to a stainless steel tray, ovendried at 110℃ for 2 hours and pulverized prior to heat treatment in the muffle furnace.

1 • 3 Experiments using Rice Husks Ash

Another series of sample mixtures containing similar molar ratios of $(CaO+MgO+K_2O)/SiO_2$, e.g. 1, 2, 2.5 and 3, were prepared using rice husks ash in place of raw rice husks. The rice husks ash prepared at the GIDLH laboratory was used in this study. Table 4 shows the amount of each raw material used for the different sample mixtures. The procedure followed in the preparation of the sample mixtures was similar to that using raw rice husks.

Table 4 . Proportionate Amount of Rice Husks Ash, Dolomitic Limestone and K_2CO_3 in the Sample Mixtures

Sample No.	Rice Husks (g)	Dolomitic Limestone (g)	K_2CO_3 (g)	K_2O (%)	Mole Ratio*
5 − 1	34.9	54.9	5.1	5.1	1
5 − 2	34.9	48.8	10.2	10.2	1
5 − 3	34.9	36.4	20.4	20.3	1
6 − 1	42.1	121.5	8.5	5.1	2
6 − 2	42.1	113.0	17.0	10.1	2
6 − 3	40.9	101.0	34.0	19.5	2
7 − 1	38.4	136.3	8.7	5.0	2.5
7 − 2	37.9	129.6	17.4	9.8	2.5
7 − 3	37.2	113.2	36.8	19.4	2.5
8 − 1	34.7	151.0	9.0	5.0	3
8 − 2	34.7	142.0	18.0	9.9	3
8 − 3	33.5	127.0	38.0	20.1	3

* $(CaO+MgO+K_2O)/SiO_2$ mole ratio

2. EXPERIMENTAL PROCEDURE

The prepared sample mixtures were each subjected to heat treatment at various temperatures in a Yamato Muffle Furnace. These experiments were carried out at 700℃, 800℃ and 900℃. Reaction times were varied at 10, 20, 30, 40 and 60 minutes.

In a typical experiment, 30g of the pulverized sample mixture was weighed into a rectangular porcelain dish, charged into the muffle furnace whicn has been pre-heated to the desired temperature, and allowed to burn. After a specified period of time, the heated product was then discharged from the furnace promptly cooled under a water bath and weighed to determine the product recovery. The dried mixture was further pulverized to 200 mesh size prior to analysis. Figure 11 shows the diagram for the heat treatment experiments using the muffle furnace.

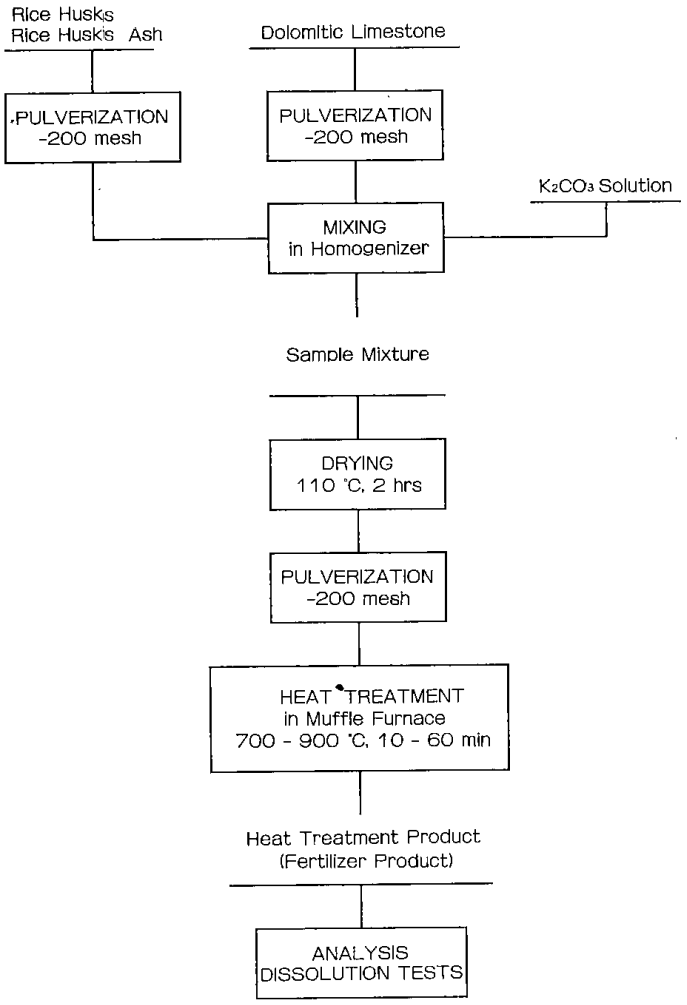

Fig. 11. Flow diagram for the preparation of slow-release type fertilizer from dolomitic limestone and rice husks.

3. ANALYSIS

3・1 Residual Carbon in the Products

The heat treated products were analyzed for residual carbon content by the JIS method. using the muffle furnace.

A 1.0g sample was weighed into a platinum crucible, charged into the muffle furnace at 925℃ and left to burn for 7 min with the lid closed. The loss in weight was reported as fixed or residual carbon.

3・2 Dissolution Test on the Products

Dissolution test on the products were carried out using 0.5N HC1, 2% citric acid and water according to the AOAC and JIS methods of analysis, of fertilizers.

3・2・1 Sample Preparation

3・2・1・a. 0.5 N HCl-Soluble and 2% Citric Acid-Soluble Components

1.0g of the heat treated product was weighed accurately into 250 mℓ-volumetric flask and added with 150 mℓ of 0.5N HC1 or 2% citric acid. The solution was shaken for 1 hour using a vertical rotary shaker at 30—40 rev/min at a constant temperature of 30℃. The

solution was then filtered immediately through a dry filter paper No.5 C using water suction.

3・2・1・b. Water-Soluble Components

1.0g of the heat treated product was weighed accurately into a 500 mℓ-volumetric flask and added 400 mℓ water. The solution was shaken for 30 minutes using a vertcal rotary shaker at 30—40 rev/min at a constant temperature of 30℃ and then diluted to mark and filtered immediately through a dry filter paper No.5C.

3・2・2 Analyses

The acid-soluble and water-soluble silicon, magnesium, calcium and potassium content of the products were analyzed according to the standard methods of analysis for each component. All of these components were expressed as oxides.

3・2・2・a. Analysis of Silicon

The acid-soluble and water-soluble silicon content of the products were determined by ICP, ion chromatograph (IC) and silico-molybdic colorimetric method.

3・2・2・b. Analysis of Calcium and Magnesium

The acid-soluble and water-soluble calcium and magnesium content of the products were determined by ICP, IC and ethylene diamine tetra acetate (EDTA) titrimetric method.

3・2・2・c. Analysis of Potassium

The acid-soluble and water-soluble potassium content of the products were determined by analysis on an ICP and IC as described previously.

3・3 X-ray Diffraction Analysis

The X-ray diffraction patterns of selected heat-treatment products were determined using a Rigaku X-ray Diffraction Analyzer. Acceleration voltage used 35KV ; current applied, 20 mA; scanning speed, 1 °/min.

The products and residue left after the dissolution tests in 0.5N HCl and water were also analyzed under similar conditions.

Identification of the compounds was done by comparison of the diffraction patterns with the ASTM powder diffraction files.

3・4 Scanning Electron Microscope Analysis

Selected samples of the heat treated products and the residues left after the acid and water dissolution tests were analyzed through a JEOL Scanning Electron Microscope Model JSM-T20 using an acceleratio voltage 1.2KV.

4. RESULTS AND DISCUSSION

4・1 Preliminary Experiments

Preliminary heat treatment studies were carried out on a mixture of dolomitic limestone and rice husks to determine their behaviour towards heat at various reaction temperatures and to monitor any reaction resulting in the formation of soluble silicate products. Sample 1 contained the following composition : 22.3% SiO_2, 49.1% CaO and 28.6% MgO. Sample 2 contained 19.8% K_2O in addition to SiO_2, CaO and MgO as shown in Table 5.

Table 5 . Chemical Composition of the Sample Mixtures in the Preliminary Experiments

Sample No.	SiO_2 (%)	CaO (%)	MgO (%)	K_2O (%)
1	22.3	49.1	28.6	
2	34.3	29.3	17.0	19.4

The results of acid and water-dissolution tests on the heat treatment products showed that the highest content of acid-soluble SiO_2 of Samle 1 was 9.14% which was obtained at 1,100℃ as shown in Table 6. Sample 2 exhibited a higher content of acid-soluble SiO_2 of 14.43% at 900℃ because of the formation of soluble silicate compounds. The results of analysis of Sample 2 is sumarized in Table 7.

Table 6 . Results of Dissolution Tests of Sample 1 in the Preliminary Experiments

Temp (℃)	Time (min)	0.5N HCl-Soluble Component (%)	2 % Citric Acid-Soluble Component (%)	Water Soluble Component (%)
		SiO_2		
900	60	0.11	2.02	—
1000	60	3.95	4.03	—
1100	60	6.14	6.51	—
1100	300	9.14	8.76	—
		MgO		
900	60	24.72	24.72	—
1000	60	25.58	24.30	—
1100	60	24.96	22.23	—
1100	300	25.98	23.70	—
		CaO		
900	60	20.12	18.74	26.96
1000	60	20.35	16.69	28.23
1100	60	21.64	14.52	25.70
1100	300	26.14	19.93	23.70

Table 7. Results of Dissolution Tests of Sample 2 in the Preliminary Experiments

Temp (℃)	Time (min)	0.5N HCl-Soluble Component (%)*	2% Citric Acid-Soluble Component (%)*	Water-Soluble Component (%)
			SiO_2	
800	60	3.86	2.99	—
900	60	22.51	19.97	—
			CaO	
800	60	10.22	9.26	18.70
900	60	17.57	13.99	12.18
			MgO	
800	60	15.91	12.19	—
900	60	17.26	16.03	—
			K_2O	
800	60	11.58	10.56	5.04
900	60	14.40	13.32	3.45

*Subtracted water-soluble values

4・2 Experiments using Rice Husks

Encouraged by the results of the preliminary findings, a series of subsequent experiments were conducted to determine the best conditions that would be suitable for the production of the slow-release silicate fertilizers. The effects of reactant composition, temperature, time and concentration of the added K_2O were studied with the end in view of maximizing the content of acid-soluble SiO_2 in the product and minimizing its content of water-soluble K_2O. The sample mixtures prepared for this study contained varying $(CaO+MgO+K_2O)/SiO_2$ mole ratios ranging between 1 and 3; their chemical compositions are shown in Table 8. The SiO_2 content of the samples ranged 26.0−59.9%; CaO, 18.3−42.2%; MgO, 10.7−24%; K_2O, 4.9−20.3%.

Table 8. Chemical Composition of the Sample Mixtures using Raw Rice Husks

Sample No.	Mole Ratio*	SiO_2 (%)	CaO (%)	MgO (%)	K_2O (%)
1 − 1	1	50.9	27.8	16.2	5.1
1 − 2	1	50.8	24.6	14.4	10.2
1 − 3	1	50.7	18.3	10.7	20.3
2 − 1	2	36.9	36.7	21.4	5.1
2 − 2	2	36.5	33.8	19.7	10.1
2 − 3	2	34.3	29.2	17.0	19.5
3 − 1	2.5	32.4	39.6	23.1	4.9
3 − 2	2.5	31.5	37.1	21.6	9.8
3 − 3	2.5	30.0	31.5	18.3	20.2
4 − 1	3	28.2	42.2	24.6	4.9
4 − 2	3	27.9	39.3	22.9	9.9
4 − 3	3	26.0	37.0	19.8	20.1

* $(CaO+MgO+K_2O)/SiO_2$ mole ratio

Heat treatment of the sample mixtures at various reaction temperatures in the muffle furnace gave products of differing contents of residual carbon, i.e., those treated at higher temperatures left behind a smaller amount of unburned carbon, as shown in Table 9. A generally decreasing trend of residual carbon content was observed in samples of increasing K_2O concentration and increasing mole ratio.

Table 9. Analysis of Residual Carbon of the Products obtained at Varying Temperatures using Raw Rice Husks

Sample No.	Mole Ratio*	K_2O (%)	Time (min)	Residual Carbon (%) 700°C	800°C	900°C
1 — 1	1	5	60	23.19	19.51	16.47
1 — 2	1	10	60	19.03	15.67	12.66
1 — 3	1	20	60	17.14	14.36	11.52
2 — 1	2	5	60	16.67	8.24	9.69
2 — 2	2	10	60	11.26	9.13	2.46
2 — 3	2	20	60	12.43	9.27	5.74
3 — 1	2.5	5	60	24.50	7.97	3.66
3 — 2	2.5	10	60	20.59	6.509	3.63
3 — 3	2.5	20	60	13.57	5.79	4.29
4 — 1	3	5	60	26.03	4.499	6.80
4 — 2	3	10	60	14.91	9.599	4.10
4 — 3	3	20	60	15.62	10.39	4.90

* $(CaO+MgO+K_2O)/SiO_2$ mole ratio

4・2・1 Results of Dissolution Tests

The results of dissolution tests on each of the heat treatment products obtained at varying reaction temperatures are summarized in Figures 12 to 22 for SiO_2, K_2O, MgO and CaO respectively. All samples were treated at 60 minutes. Analysis results of 0.5N HCl, 2% citric acid and water-soluble components exhibited various trends with respect to the various parameters. The values presented for the 0.5N HCl and 2% citric acid-soluble K_2O and CaO have been subtracted of water-soluble values. The products do not contain water-soluble contents of SiO_2 and MgO.

4・2・1・a. Effect of Mole Ratio

Figure 12 shows the effect of varying mole ratios of $(CaO+MgO+K_2O)/SiO_2$ on the concentration of 0.5N HCl-soluble and 2% citric acid-soluble SiO_2 in the products. Typical trends are shown for samples containing 20% K_2O. Results show that the formation of acid-soluble SiO_2 is very much affected by differences in mole ratio. At a reaction temperature of 900℃, increasing this mole ratio from 1 to 2 produced a sudden increase of acid-soluble SiO_2, from 2.86% to 22.5%. With further increase of mole ratio, the content of acid-soluble SiO_2, gradually drops until it reaches a value of 10.59% at a mole ratio of 3. At 800℃, values of SiO_2 obtained are much lower than those at 900℃ ; at this temperature, the highest attainable content of SiO_2 was only 8.39%. This value was observed at a mole ratio of 2.5.

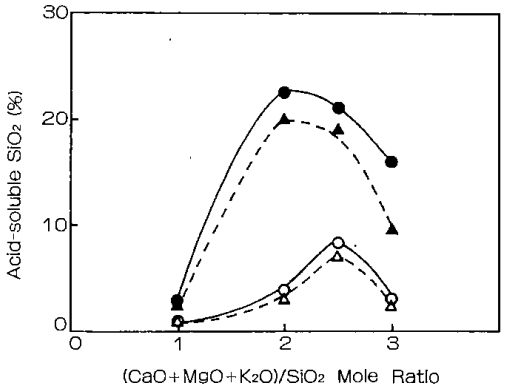

Fig. 12. Effect of mole ratio on the 0.5N HCl-soluble and 2% citric acid-soluble SiO_2 content of the product
○ : 0.5N HCl-soluble SiO_2 at 800°C
● : 0.5N HCl-soluble SiO_2 at 900°C
△ : 2% citric acid-soluble SiO_2 at 800°C
▲ : 2% citric acid-soluble SiO_2 at 900°C

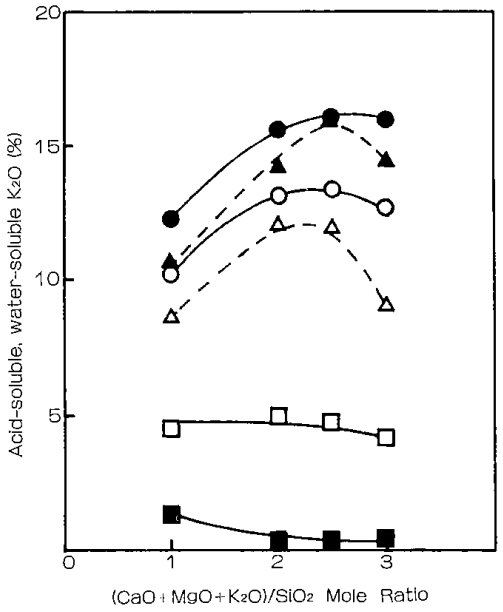

Fig. 13. Effect of (CaO+MgO+K_2O)/SiO_2 mole ratio on the 0.5N HCl-soluble, 2% citric acid-soluble and water-soluble K_2O content of the product

○ : 0.5N HCl-soluble K_2O at 800°C
● : 0.5N HCl-soluble K_2O at 900°C
△ : 2% citric acid-soluble K_2O at 800°C
▲ : 2% citric acid-soluble K_2O at 900°C
□ : water-soluble K_2O at 800°C
■ : water-soluble K_2O at 900°C
K_2O content of starting material . 20%

Figure 13 shows that the highest value of acid-soluble K_2O is 16.12% at a mole ratio of 2.5.

Water-soluble K_2O, on the other hand, does not vary much with changes in mole ratio. Lowest value observed was 1.23% in products obtained at 900℃.

The content of acid-soluble MgO and CaO of the heat treatment products also shows an increasing trend of values with increasing mole ratios. Maximum values are observed at mole ratios of 2 and 2.5 for CaO as shown in Figure 14 and 15. At higher mole ratios, a decrease of acid-constituents is indicated at a temperature of 900℃.

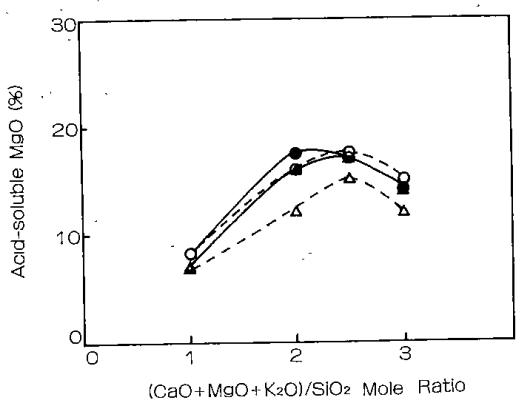

Fig. 14. Effect of (CaO+MgO+K_2O) / SiO_2 mole ratio on the 0.5N HCl-soluble and 2% citric acid-soluble MgO content of the product
○ : 0.5N HCl-soluble MgO at 800°C
● 0.5N HCl-soluble MgO at 900°C
△ : 2% citric acid-soluble MgO at 800°C
▲ : 2% citric acid-soluble MgO at 900°C

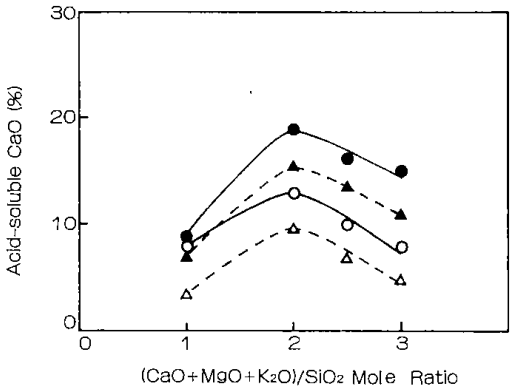

Fig. 15. Effect of $(CaO+MgO+K_2O)/SiO_2$ mole ratio on the 0.5N HCl-soluble and 2% citric acid-soluble CaO content of the product
○ : 0.5N HCl-soluble CaO at 800℃
● : 0.5N HCl-soluble CaO at 900℃
△ : 2% citric acid-soluble CaO at 800℃
▲ : 2% citric acid-soluble CaO at 900℃

4・2・1・b. Effect of K_2O Concentration

The addition of potassium in the form of K_2CO_3 to the mixture of dolomitic limestone and rice husks has been shown to facilitate the formation of soluble silicate compounds at temperatures lower than 1000℃ as previously indicated in the preliminary experiments. Figure 16 shows the trend of 0.5N HCl and 2% citric acid-soluble SiO_2 with increasing K_2O concentration. Comparative trends are illustrated for samples with mole ratios of 2 and 2.5, at temperatures of 800℃ and 900℃. As the K_2O in the sample increases, a rapid increase in acid-soluble SiO_2 is indicated particularly at 900℃, i.e. for the sample containing a $(CaO+MgO+K_2O)/SiO_2$ mole ratio of 2.0, an increase of K_2O concentration from 5 to 20% produced a subsequent increase in 0.5N HCl-soluble SiO_2 from 4.94% to 22.5%. At 800℃, a slight increase of values is observed with increased K_2O concentration, but not as pronounced as there at 900℃.

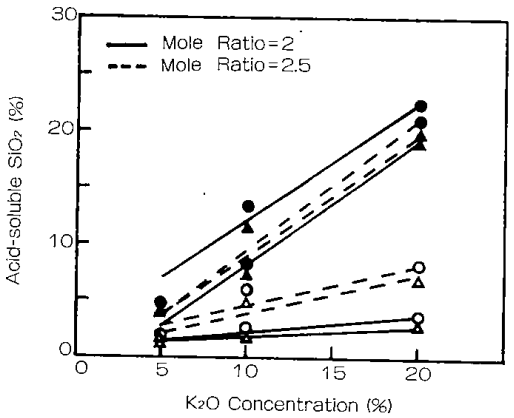

Fig.16 Effect of K_2O concentration on the 0.5N HCl-soluble and 2% citric acid-soluble SiO_2 content
○:0.5N HCl-soluble SiO_2 at 800℃
●:0.5N HCl-soluble SiO_2 at 900℃
△:2% citric acid-soluble SiO_2 at 800℃
▲:2% citric acid-soluble SiO_2 at 900℃

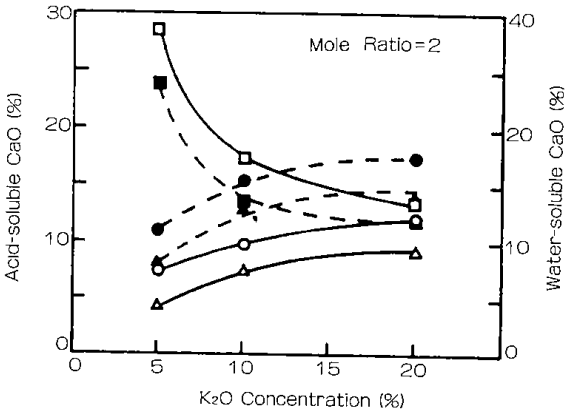

Fig 17 Effect of K_2O concentration on the 0.5N HCl-soluble, 2% citric acid-soluble and water-soluble CaO content
○ 0.5N HCl-soluble CaO at 800℃
●:0.5N HCl-soluble CaO at 900℃
△:2% citric acid-soluble CaO 800℃ at 800℃
▲:2% citric acid-soluble CaO at 900℃
□:Water-soluble CaO at 800℃
■:Water-soluble CaO at 900℃

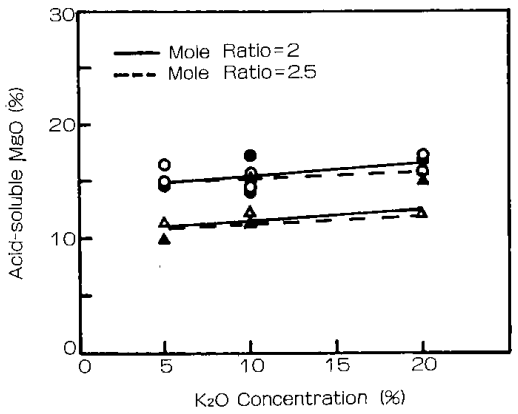

Fig.18 Effect of K_2O concencentration on the 0.5N HCl-soluble and 2% citric acid-soluble MgO content
○:0.5N HCl-soluble MgO at 800℃
●:0.5N HCl-soluble MgO at 900℃
△:2% citric acid-soluble MgO at 800℃
▲:2% citric acid-soluble MgO at 900℃

The effect of K_2O concentration on acid-soluble and water soluble CaO content is shown in Figure 17 for samples containing mole ratio 2. As observed with SiO_2 values, a continuous increase of acid-soluble CaO is obtained with increasing K_2O concentration, especially at 900℃ ; the highest value obtained was 17.50%. Water-soluble CaO is decreased with increased K_2O concentration.

The content of acid-soluble MgO of the products was not affected to a great extent with changes in K_2O as shown in Figure 18 0.5N HCl-soluble and 2% citric acid-soluble MgO reach maximum values of 17.36% and 12.50% respectively at 800℃ using 20% K_2O.

4・2・1・c. Effect of Temperature

The reaction of dolomitic limestone, rice husks and K_2CO_3 has been observed to occur at a temperature of 750℃ as previously mentioned. The influence of the reaction temperature on the soluble constituents of the product is discussed here.

The influence of reaction temperature on the acid-soluble SiO_2 content of the products is best illustrated in Figure 19 for samples containing mole ratios of 2 and 2.5. Both 0.5N HCl and 2% citric acid-soluble SiO_2 show an increasing trend of values with increased temperature, with highest values at 900℃. At a mole ratio of 2, for instance, raising the temperature from 800℃ to 900℃ produced a subsequent increase in HCl-soluble SiO_2 from 3.87% to 22.51%.

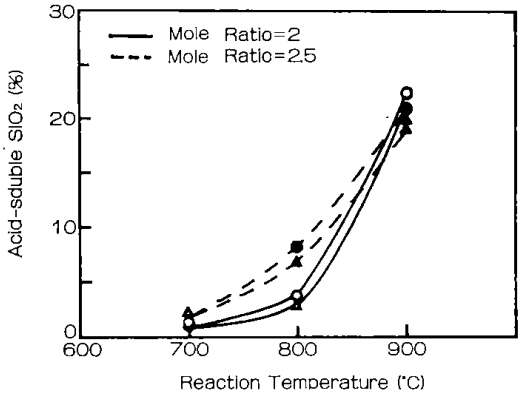

Fig.19 Effect of temperature the 0.5N HCl-SiO_2 citric acid-soluble SiO_2 content in the products obtained using rice husks as source of silica
O, :0.5N HCl-soluble SiO_2
△, ▲:2% citric acid-soluble SiO_2

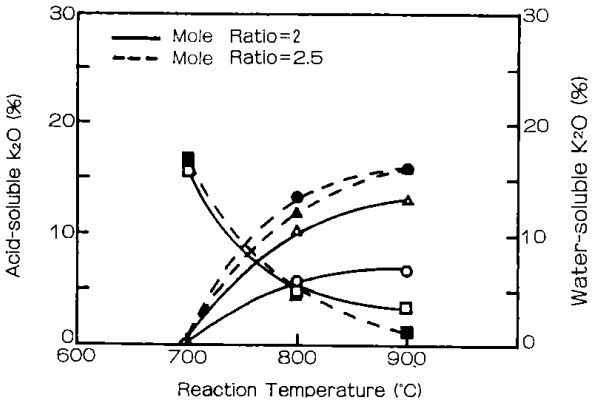

Fig.20 Effect of temperature on the 0.5N HCl-soluble 2% citric acid-solube and water-soluble K_2O content
O, ●:0.5N HCl-soluble k_2O
△, ▲:2% citric acid-soluble K_2O
□, ■:Water-soluble k_2O

Similarly, the content of acid-soluble K_2O was observed to be generally in the upward trend with respect to increasing temperatures as reflected in Figure 20.

The contnet of acid-soluble MgO in the products was affected greatly between 700℃ and 800℃ but not affected at 800~900℃ as shown in Figure 21. On the other hand, acid -soluble CaO is shown to increase temperature ; the highest value obtained is 21.62% as can be seen from Figure 22. The content of water-soluble CaO, however, exhibits a maximum at 800℃ and then drops at 900℃.

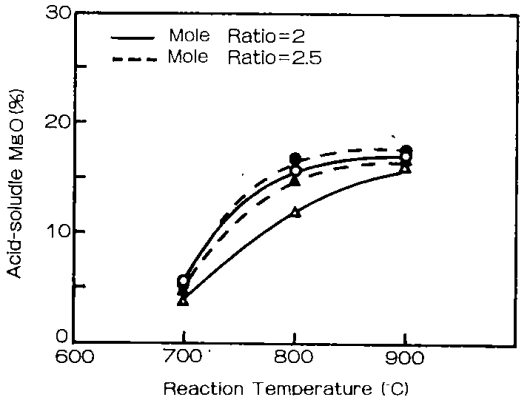

Fig.21 Effect of temperature on the 0.5N HCl-soluble and 2% citric acid-soluble MgO content
O, ●:0.5N HCl-soluble MgO
△, ▲:2% citric acid-soluble MgO

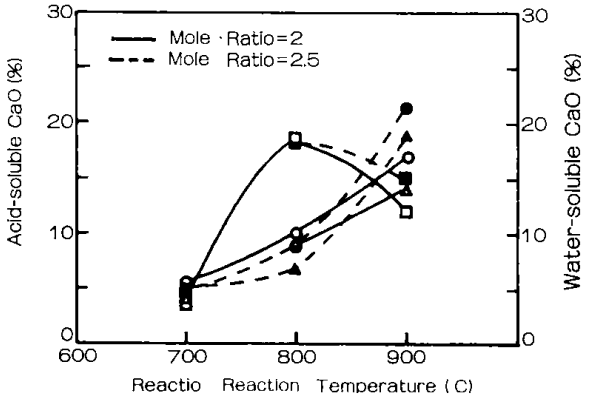

Fig.22 Effect of temperature on the 0.5N HCl-soluble . 2% citric acid-soluble and water-soluble CaO content
O, ●:0.5N HCl-soluble CaO
△, ▲:2% citric acid-soluble CaO
□, ■:Water-soluble CaO

4・2・1・d. Effect of Reaction Time

For the studies on the effect of reaction time, samples with mole ratios of 2.0 and 2.5 were investigated.

For SiO_2, K_2O, MgO and CaO respectively, the trend of HCl-soluble SiO_2 content in the products at different reaction times is shown in Figure 23. The graph illustrates that the acid-soluble SiO_2 increases as reaction proceeds from 10 to 30minutes and then remains constant with further increase in reaction time. A similar trend of data is also observed with acid-soluble K_2O and MgO as reflected in Figures 24 and 25 respectively. The values

of water-soluble K_2O exhibit a decreasing trend from 10 to 30 minutes and then stabilize between 30 to 60 minutes.

The acid-soluble CaO content of the product, however, exhibited a different trend. The values are observed to increase between 10 to 20 minutes and remain constant up to 40 minutes and then increases as reaction time is lenghtened to 60 minutes. This is shown in Figure 26.

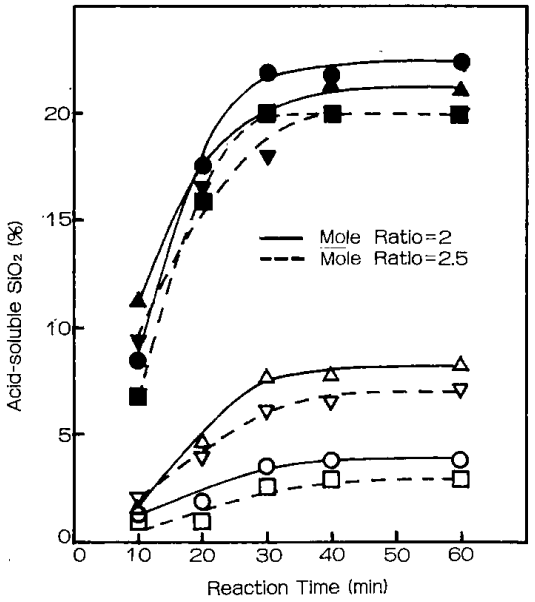

Fig.23 Effect of reaction time on the 0.5N HCl-soluble and 2% citric acid-soluble SiO_2 content
△, ○:0.5N HCl-soluble SiO_2 at 800°C
●, ▲0.5N HCl-soluble SiO_2 SiO_2 at 900°C
▽, □:2% citric acid-soluble SiO_2 at 800°C
■, ▼:2% citric acid-soluble SiO_2 at 900°C
K_2C content of staring material :20%

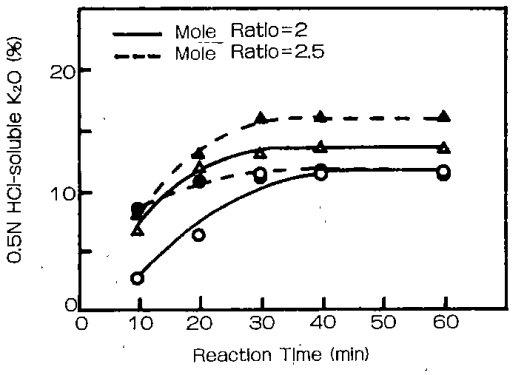

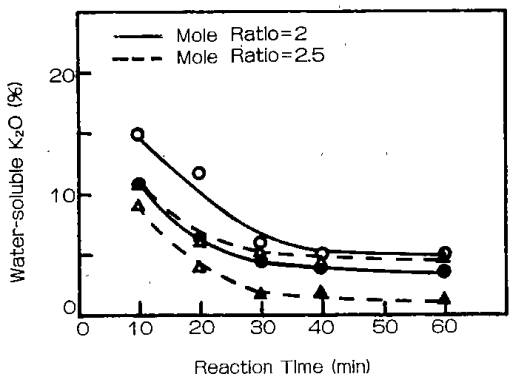

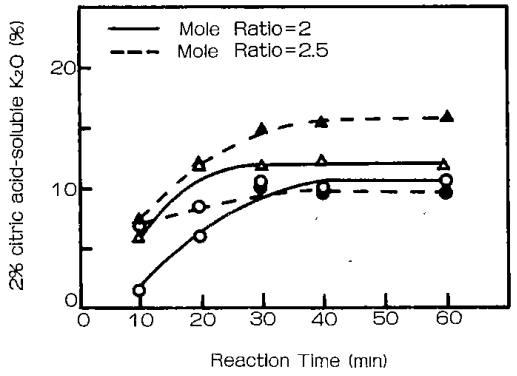

Fig.24 Effect of reaction tn the 0.5N HCl-soluble, 2% citric acid-soluble and water-soluble K_2O content
○, △:800°C
●, ▲:900°C
K_2O content of starting material :20%

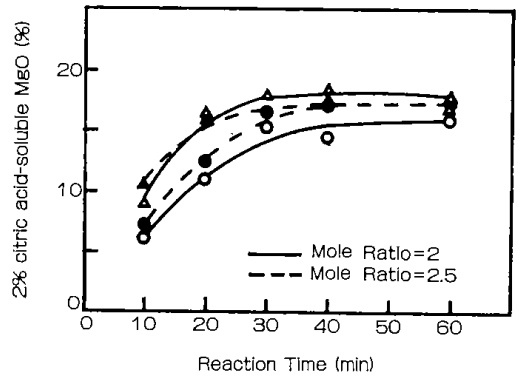

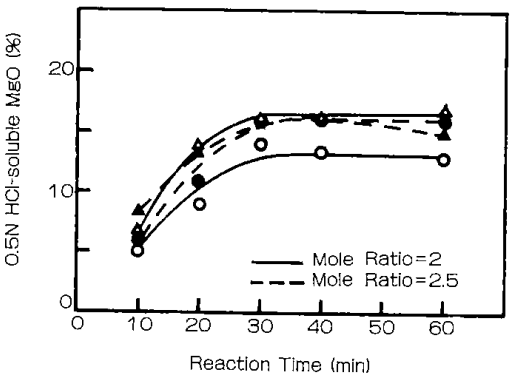

Fig.25 Effect of reaction time on the 0.5N HCl-soluble and 2% citric acid-soluble MgO content
○, △:800°C
●, ▲:900°C
K_2O content of starting material :20%

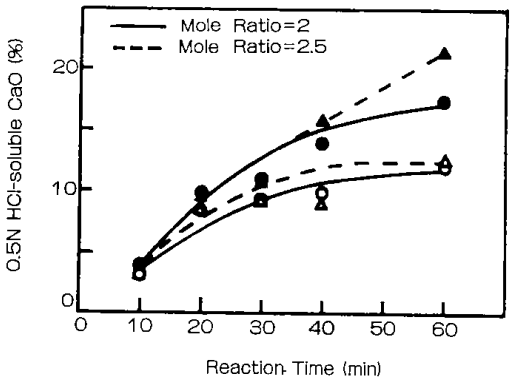

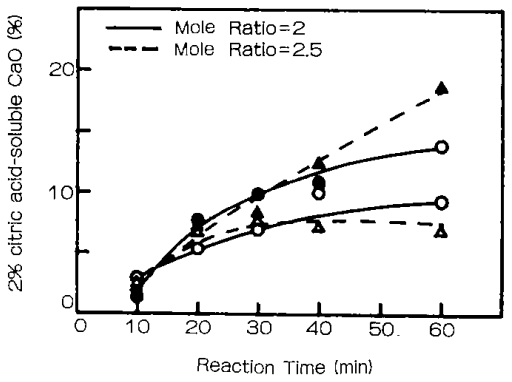

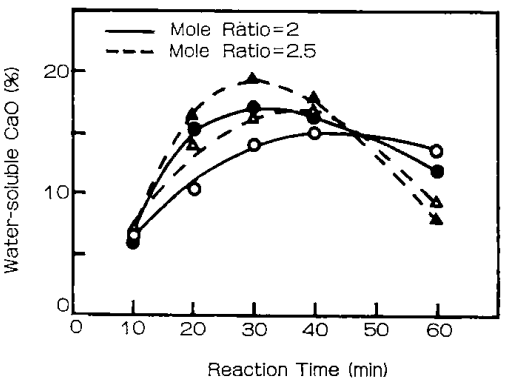

Fig.26 Effect of reaction time on the 0.5N HCl-soluble, 2% citric acid-soluble and water-soluble CaO content
○, △:800°C
●, ▲:900°C

4・2・2 X-ray Analysis

The formation of silicate compounds after the heat treatment of the sample mixtures at varying temperatures was monitored by X-ray analysis of the product. Figure 27 shows the X-ray diffraction pattern of sample 2 — 3 (mole ratio= 2), products obtained at 700℃ 800℃ and 900℃ for 60 minutes. At 900℃, the presence of silicates is clearly indicated by the appearance of peaks corresponding to K_2CaSiO_4 and K_2MgSiO_4 among others. At 700℃ and 800℃, the formation of these silicates is not indicated.

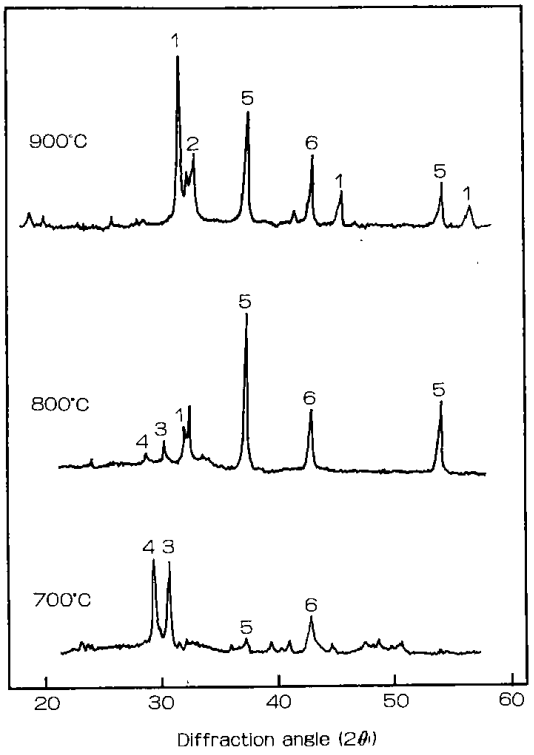

Fig.27 X-ray diffraction pattern of the products obtained from samples of varying temperature:
$(CaO+Mg+K_2O)/SiO_2$ mole ratio=2, K_2O=20%
1:K_2CaSiO_4, 2:K_2MgSiO_4, 3:$CaMg(CO_3)_2$, 4:α-Ca_2SiO_4
5:CaO, 6:MgO

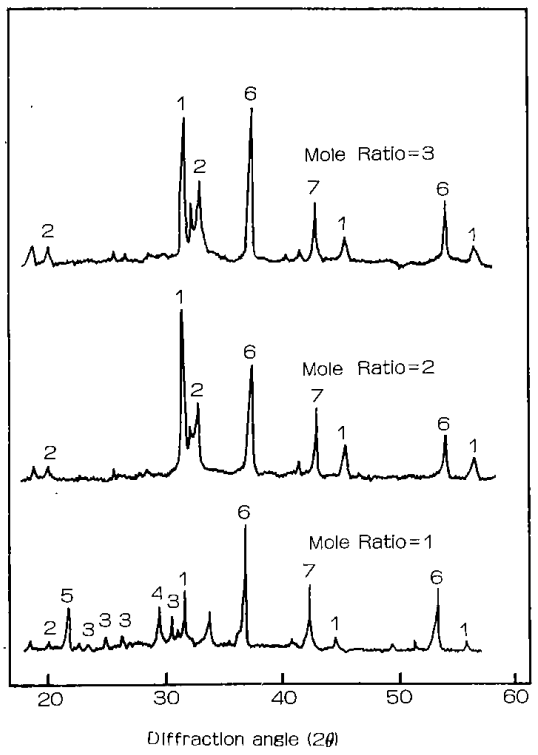

Fig.28 X-ray diffraction pattern of the products obtained from samples of varying $(CaO+MgO+K_2O)$ SiO_2 mole ratio; at 900°C, K_2O=20%
1:K_2CaSiO_4, 2:K_2MgSiO_4, 3:α-$CaSiO_3$, 4:α-Ca_2SiO_4
5:Cristobalite, 6:CaO, 7:MgO

Figure 28 shows the comparative X-ray pattern of the heat treatment products obtained at 900℃ using different mole ratios of $(CaO+MgO+K_2O)/SiO_2$. The presence of various species of silicate compounds is indicated at different ratios which explains the discrepancies obtained in the dissolution tests. The formation of α-Ca_2SiO_4 is observed at a mole ratio of 2 in addition to K_2MgSiO_4 and K_2CaSiO_4 which are also formed at a mole ratio of 3.

The X-ray analysis of the acid-insoluble residue left after the dissolution tests in 0.5N HCl is illustrated in Figure 29. Different patterns are obtained with the products of different mole ratios, i.e., the residue from the product produced from a mole ratio of 1 still shows the presence of insoluble crystalline materials, particularly cristobalite. This explains the lower results of dissolution tests with this product, compared with those obtained at mole ratio 2.

4・2・3 Scanning Electron Microscopy

The scanning electron micrograph of a representative of 0.5N HCl and water insoluble residue of the product after the dissolution tests is shown in Figure 30 obtained at 900℃.

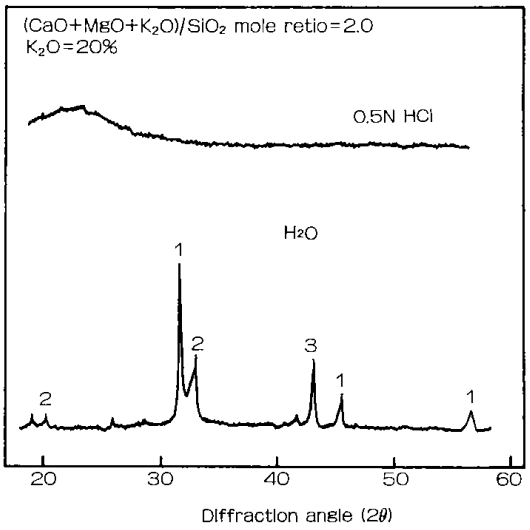

Fig.29 X-ray diffraction pattern of the 0.5N HCl and water insoluble residue of the products obtained at 900℃
1:K_2CaSiO_4, 2 K_2MgSiO_4 3:MgO

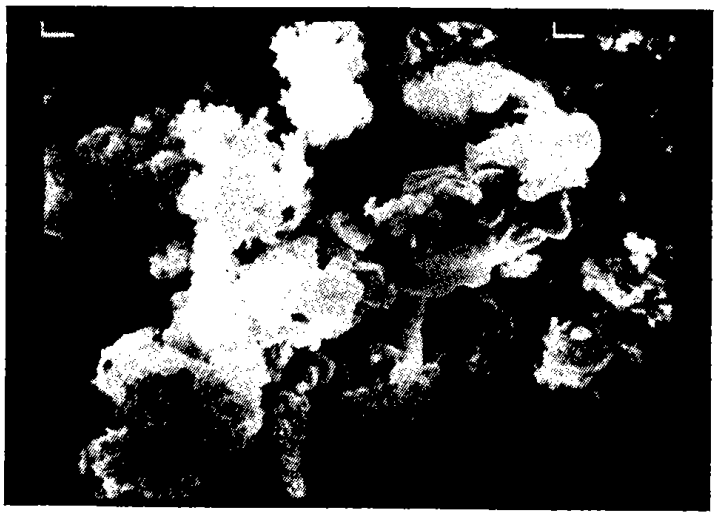

Magnification x 5000 [10μm]

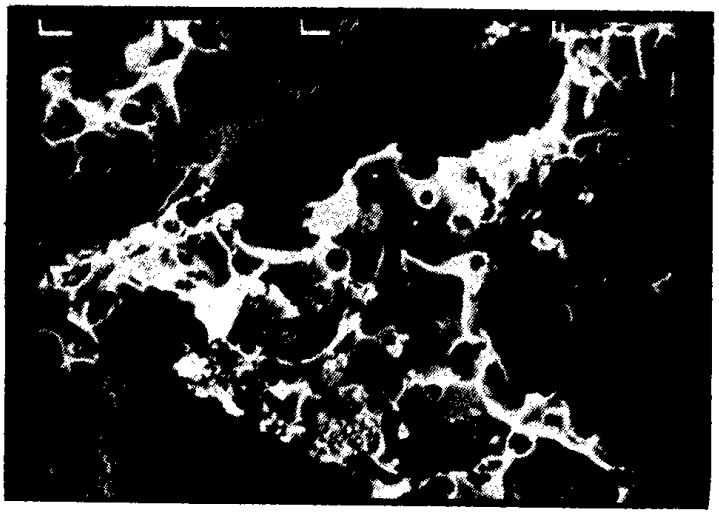

Magnification x 2500 [10μm]

Fig.30 Surface of the heat treated product at 900℃ and the acid residue in 0.5N HCl in Scanning Electoron Microscope

4・3 Experiments using Rice Husks Ash

Comparative experiments ware conducted using rice husks ash in instead of rice husks as a source of silicon. The series of sample mixtures prepared contained similar chemical compositions as those used in the earlier runs on rice husks ash as shown in Table.10.

Table.11 summarizes the analysis of residual carbon of the products.

Table 10. Chemical Composition of the Sample Mixtures using Rice Husks Ash

Sample No.	Mole Ratio	SiO_2 (%)	CaO (%)	MgO (%)	K_2O (%)
5 − 1	1	51.1	27.7	16.1	5.1
5 − 2	1	50.0	24.6	14.3	10.2
5 − 3	1	50.8	18.3	10.7	20.3
6 − 1	2	36.9	36.7	21.4	5.1
6 − 2	2	36.5	33.8	19.7	10.1
6 − 3	2	34.3	29.2	17.0	19.5
7 − 1	2.5	32.2	39.6	23.1	5.0
7 − 2	2.5	31.5	37.1	21.6	9.9
7 − 3	2.5	30.0	315.	18.3	20.0
8 − 1	3	28.2	42.2	24.6	4.9
8 − 2	3	27.9	39.3	22.9	9.9
8 − 3	3	26.0	34.6	19.8	20.1

* $(CaO+MgO+K_2O)/SiO_2$ mole ratio

Table 11. Analysis of Residual Carbon of the Products obtained at Varying Temperatures using Rice Husks' Ash

Sample No.	Mole Ratio*	K_2O (%)	Time (min)	Residual Carbon (%) 700°C	800°C	900°C
5 − 1	1	5	60	19.4	7.02	5.54
5 − 2	1	10	60	11.87	6.47	4.14
5 − 3	1	20	60	8.27	4.94	2.21
6 − 1	2	5	60	21.25	11.68	4.09
6 − 2	2	10	60	14.24	5.47	3.12
6 − 3	2	20	60	12.19	8.03	3.91
7 − 1	2.5	5	60	22.93	10.67	4.93
7 − 2	2.5	10	60	16.40	9.17	2.55
7 − 3	2.5	20	60	14.29	7.43	6.25
8 − 1	3	5	60	22.14	6.69	11.15
8 − 2	3	10	60	18.75	5.02	4.98
8 − 3	3	20	60	15.8	11.41	2.45

* $(CaO+MgO+K_2O)/SiO_2$ mole ratio

Dissolution tests of the products are summarized in Table 12, 13, 14 and 15 for SiO_2, K_2O, MgO and CaO, respectively. In comparison with the previous results, the values obtained for acid-soluble and water-soluble components exhibited similar trends of values with respect to changes in temperature, mole ratio and concentration of K_2O in the sample.

Table 12. Comparative Analysis of the Acid-Soluble Silicon Content of the Heat Treatment products using Rice Husks Ash

Sample	Temp (℃)	Time (min)	0.5N HCl-Soluble SiO_2 (%)	2% Citric Acid-Soluble SiO_2 (%)
5 − 1	700	60	0.18	0.22
	800	60	0.45	0.36
	900	60	3.66	3.17
5 − 2	700	60	0.38	0.31
	800	60	1.06	0.87
	900	60	4.09	3.93
5 − 3	700	60	1.11	0.74
	800	60	2.08	1.93
	900	60	3.13	2.91
6 − 1	700	60	0.95	0.80
	800	60	1.24	1.01
	900	60	4.65	3.75
6 − 2	700	60	1.09	0.85
	800	60	2.54	1.62
	900	60	8.11	7.16
6 − 3	700	60	2.57	2.00
	800	60	3.99	3.11
	900	60	23.14	20.70
7 − 1	700	60	1.36	0.91
	800	60	1.73	0.99
	900	60	4.08	3.55
7 − 2	700	60	1.69	0.91
	800	60	5.89	4.49
	900	60	12.70	10.59
7 − 3	700	60	1.39	1.01
	800	60	8.00	7.02
	900	60	20.09	18.16
8 − 1	700	60	0.94	0.49
	800	60	1.38	0.88
	900	60	3.65	3.02
8 − 2	700	60	1.12	0.57
	800	60	2.88	1.96
	900	60	5.09	4.38
8 − 3	700	60	1.14	1.00
	800	60	3.03	3.05
	900	60	12.06	11.62

Table 13. Comparative Analysis of the Acid-Soluble and Water Soluble Potassium Content of the Heat Treatmen Products using Rice Husks Ash

Sample No.	Temp (℃)	Time (min)	0.5N HCl-Soluble K_2O (%)*	2% Citric Acid-Soluble K_2O (%)*	Water-Soluble K_2O (%)
5 — 1	700	60	0.22	—	3.66
	800	60	1.35	1.19	2.92
	900	60	—	—	2.88
5 — 2	700	60	0.32	—	8.37
	800	60	4.57	4.53	4.80
	900	60	0.20	0.09	4.61
5 — 3	700	60	6.65	6.37	5.49
	800	60	17.11	16.20	0.57
	900	60	11.57	11.17	3.82
6 — 1	700	60	0.06	—	3.59
	800	60	1.21	1.15	2.66
	900	60	1.60	1.54	2.60
6 — 2	700	60	0.80	0.05	7.00
	800	60	5.72	5.31	2.70
	900	60	7.78	7.46	0.73
6 — 3	700	60	0.45	0.47	16.55
	800	60	11.68	10.33	5.75
	900	60	13.86	13.64	2.27
7 — 1	700	60	—	—	3.49
	800	60	1.74	1.57	2.16
	900	60	3.63	3.33	0.42
7 — 2	700	60	0.18	0.07	8.12
	800	60	5.33	4.66	2.84
	900	60	7.16	6.23	1.10
7 — 3	700	60	0.26	—	18.11
	800	60	13.58	13.52	4.70
	900	60	16.45	16.18	1.14
8 — 1	700	60	—	—	3.94
	800	60	1.65	0.80	2.25
	900	60	3.50	3.33	0.55
8 — 2	700	60	0.03	—	8.61
	800	60	5.06	4.97	3.03
	900	60	7.09	6.96	1.06
8 — 3	700	60	0.48	0.28	16.19
	800	60	10.89	10.76	6.27
	900	60	17.33	16.30	0.72

*Subtracted water-soluble values

Table 14. Comparative Analysis of the Acid-Soluble Magnesium Content of the Heat Treatment products using Rice Husks Ash

Sample No.	Temp (℃)	Time (min)	0.5N HCl-Soluble MgO (%)	2% Citric Acid-Soluble MgO (%)
5 — 1	700	60	4.02	2.96
	800	60	11.13	9.44
	900	60	11.96	10.10
5 — 2	700	60	6.16	3.64
	800	60	8.69	4.18
	900	60	13.57	12.89
5 — 3	700	60	4.88	3.64
	800	60	10.11	8.08
	900	60	10.09	9.43
6 — 1	700	60	4.93	3.37
	800	60	13.01	12.70
	900	60	14.26	10.03
6 — 2	700	60	5.14	3.55
	800	60	14.67	12.31
	900	60	13.06	11.03
6 — 3	700	60	6.25	4.26
	800	60	16.44	12.47
	900	60	19.02	16.83
7 — 1	700	60	4.70	4.17
	800	60	15.22	14.75
	900	60	13.23	11.04
7 — 2	700	60	5.39	4.99
	800	60	15.33	14.00
	900	60	13.44	11.08
7 — 3	700	60	5.54	4.94
	800	60	18.27	16.53
	900	60	17.10	15.14
8 — 1	700	60	5.50	4.62
	800	60	14.62	10.11
	900	60	14.92	11.03
8 — 2	700	60	5.36	4.05
	800	60	14.45	13.80
	900	60	15.00	13.86
8 — 3	700	60	5.20	3.84
	800	60	14.70	12.29
	900	60	17.82	16.22

Table 15. Comparative Analysis of the Acid-Soluble and Water-Soluble Calcium Content of the Heat Treatment Products using Rice Husks Ash

Sample No.	Temp (℃)	Time (min)	0.5N HCl-Soluble CaO (%)*	2% Citric Acid-Soluble CaO (%)*	Water-Soluble CaO (%)
5 − 1	700	60	2.24	0.78	1.79
	800	60	7.11	4.29	14.56
	900	60	7.81	5.33	15.15
5 − 2	700	60	2.47	1.04	2.97
	800	60	4.41	2.92	8.94
	900	60	8.10	5.46	10.84
5 − 3	700	60	4.75	4.52	4.24
	800	60	7.93	3.56	8.58
	900	60	8.94	6.90	5.73
6 − 1	700	60	3.79	1.86	3.15
	800	60	7.13	4.40	13.22
	900	60	10.77	8.08	10.87
6 − 2	700	60	4.57	2.37	4.18
	800	60	10.18	8.01	16.44
	900	60	14.60	12.11	13.09
6 − 3	700	60	6.00	4.14	2.48
	800	60	12.84	9.65	13.15
	900	60	18.91	15.35	11.56
7 − 1	700	60	4.44	3.49	4.11
	800	60	4.75	3.06	7.03
	900	60	6.76	6.05	6.20
7 − 2	700	60	2.16	1.70	5.52
	800	60	10.01	8.58	17.05
	900	60	13.19	25.37	13.79
7 − 3	700	60	3.73	1.28	6.14
	800	60	9.78	6.80	19.20
	900	60	16.19	13.46	13.07
8 − 1	700	60	3.91	1.16	4.88
	800	60	10.7	7.15	14.10
	900	60	16.72	14.74	12.41
8 − 2	700	60	3.89	1.36	6.70
	800	60	10.05	8.68	16.09
	900	60	14.16	12.09	13.91
8 − 3	700	60	4.36	2.17	3.88
	800	60	7.79	4.84	14.37
	900	60	14.98	10.99	13.03

*Subtracted water-soluble values

The effect of temperature on the acid-soluble SiO_2 content in products obtained using rice husks ash is shown in Figure 31.

Compared with the data using rice husks (Fig. 19), there is very little difference between the two materials, rice husks and rice husks ash.

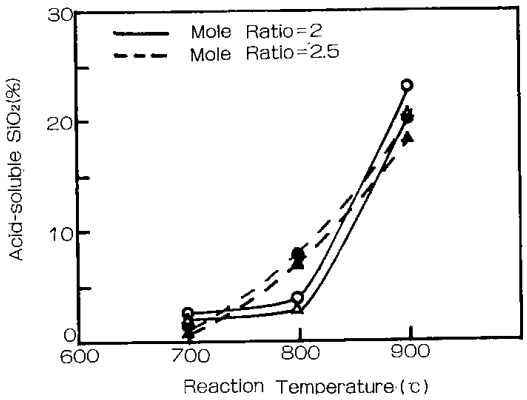

Fig.31 Effect of temperature on the 0.5N HCl-soluble and 2% citric acid-soluble SiO_2 content in the products obtained using rice husks ash as source of silica

These results seem to prove that even as the source of silica takes the form of a rice husks or rice husks ash, similar results would be obtained since both materials contain amorphous types of silica.

5. CONCLUSIONS

Basic heat treatment studies have been conducted on sample mixtures of dolomitic limestone, rice husks and K_2CO_3 with the view towards establishing the optimum conditions required in the production of silicate products exhibiting the properties of a slow-release fertilizer. Studies made on the muffle furnace were centered on determining the effect of varying conditions of reaction temperature, time, reactant mole ratio and concentration of added K_2O on the products. Results are summarized as follows :

1. Variations in the chemical composition of the reactants in terms of mole ratio $(CaO+MgO+K_2O)/SiO_2$, resulted in the formation of products of varying properties. Maximum values of acid-soluble SiO_2, K_2O, MgO and CaO were formed at mole ratios of 2 and 2.5.
2. The addition of K_2CO_3 to the reaction mixture of dolomitic limestone and rice husks resulted in the lowering of the reaction temperature and a subsequent increase in the content of acid-soluble constituents of the heat treatment products. This latter effect was enhanced with higher K_2O concentrations.
3. The effect of reaction temperature is best observed by the formation of acid-soluble SiO_2, which exhibited a maximum value of 22.51% at 900℃.
4. The present study revealed that the reaction seems to be optimized at a reaction time of 30 minutes and that lengthening the time to 60 minutes produces very slight differences.
5. Comparative studies using raw rice husks and rice husks ash as sources of silica revealed similar trends of values at parallel conditions even as the resulting products contained varying amounts of residual carbon. Since both rice husks and rice husks ash contain amorphous silica, both materials proved to be good starting materials for the production of silicate materials.
6. The results of the study proved that it is indeed possible to produce silicate products from dolomitic limestone and rice husks which exhibit properties of a slow-release fertilizer.

石炭液化残渣とガス化灰とによるハイブリッド粒子のガス化

田崎米四郎・千葉　繁生・弓山　翠・武田　詔平
本間　専治・北野　邦尋・河端　淳一

石炭液化の残渣は液化油の精製プロセスにもよるが，遠心分離機残渣と蒸留残渣からなっている。遠心分離機残渣は固体粒子を含み，しかも高粘度であるためハンドリングも容易でなくその処理は未解決の課題である。また，蒸留残渣は常温で固体であるが約100℃の加熱で軟化し始めるため，処理装置内での流動化が困難である。一方，石炭の高圧流動層ガス化炉からの溢流灰および飛び出し粒子は数％～30数％の未反応炭素分を含んでおり，炭素転換率が低いことが流動層ガス化炉の欠点の一つとされている。石炭液化に必要な水素は石炭のガス化により製造することが検討されており，具体的方法も提案されているが石炭利用技術のガス化，液化を一つのクローズドシステムとして位置付け，全体として炭素転換率を高くしようとする試みはなされていない。著者らは以上の観点から実験を重ね，石炭液化残渣とガス化灰とを混合するとハンドリングが容易で流動化可能なハイブリッド粒子となることを見いだした。本研究では，このハイブリッド粒子を常圧の流動層により酸素と水蒸気でガス化し，生成ガス組成および炭素転換率等に及ぼすガス化温度，ガス化剤の酸素濃度の影響を調べた。

実験試料

石炭液化残渣は日本鋼管の2.4トン／日石炭液化プラントの遠心分離機残渣および重質油の真空蒸留残渣である。Fig. 1に示した遠心分離機残渣は触媒を含み灰分50%，未反応分15%，中重油分35%であり，粘度は80℃において約1000cPである。真空蒸留残渣はFig. 2に示すように数mmから数cmの大きさで（以下フレークピッチと呼ぶ），常温では固体であるが，約100℃の加熱で軟化し，灰分10%，元素分析による炭素成分は76%である。ガス化灰は北開試の１トン／日　高圧流動層ガス化炉によって1000℃のガス化条件で生成した溢流灰であり，灰分が約80%，BET表面積が120～220 m^2／gである。混合粒子（ハイブリッド粒子）の調整はまず遠心分離機残渣とガス化灰を重量比で１対１に配合し，次に50℃に加熱したアスファル

Fig. 1 Coal liquefaction residue from centrifugal separator

Fig. 2 Flake pitch from coal liquefaction plant

トミキサーで数分間攪拌することによって行った。この方法によって遠心分離機残渣はガス化灰粒子に容易に付着，分散しハンドリングが可能な流動性の良い粒子となった。フレークピッチを流動炉で処理するためには5㎜以下に粉砕する必要があるが，そのまま通常の粉砕機にかけるとピッチ内部から侵出した油が粉砕機に付着するという難点がある。しかし粒径1.68㎜以下のガス化灰をピッチに対し重量で2.5倍混合することによって，粉砕中に侵出した油分がガス化灰に付着し，ピッチを問題なく容易に粉砕できることがわかった。この混合試料を300℃に加熱したダブルスクリュウフィダーで供給すると，供給管内で部分的に溶融したピッチがガス化灰に付着し，流動化に適した粒子性状となって流動炉への供給が可能になった。以上の前処理による遠心分離機残渣とガス化灰との混合粒子およびフレークピッチとガス化灰との混合粒子（ハイブリッド粒子）の形状はFig. 3のようにほとんど同じである。ハイブリッド粒子は調整前の元のガス化灰粒子より粒径が大きくなる。Fig. 4に遠心分離機残渣のハイブリッド粒子とガス化灰粒子の粒径分布を示す。また，2種類のハイブリッド粒子の元素分析値，発熱量，かさ密度，流動化開始速度をTable 1に示す。

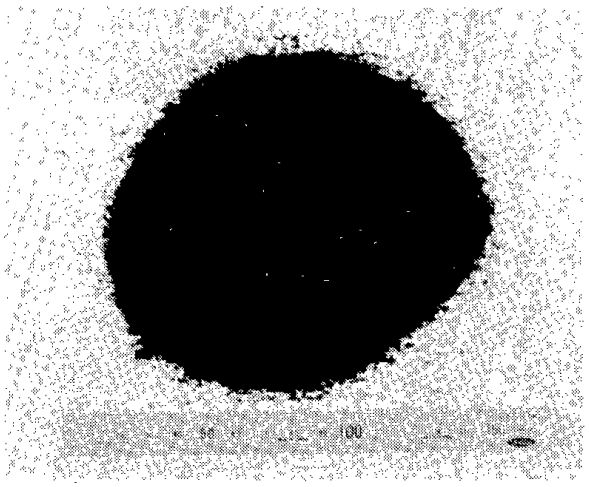

Fig. 3 Hybrid particles

実験装置および方法

流動層ガス化装置のフローシートをFig. 5に示す。流動炉本体は内径0.108m，全長1.15mのSUS316製である。流動媒体として0.35～0.50㎜の硅砂（U_{mf}＝0.19m／s）を使用し，炉内ガス線速度は0.57m／sとした。ガス化温度T_bは混合試料の供給量を増減するオンオフ制御によって±5℃以内にコントロールした。ガス化後の粒子はガス分散板の上0.4mの高さの溢流管から排出される。

実験結果および考察

遠心分離機残渣とのハイブリッド粒子に対し，ガス化剤中の酸素濃度を20%としガス化温度を変えた場合の生成ガスの組成，発熱量H_h，および炭素転換率C_Gの結果をFig. 6に示す。ガス化温度の上昇と共にC_Gは大きくなるが，高温を維持するために燃焼反応の割合が大きくなってCO_2濃度が増加する。しかし，CO，H_2合わせて約60%であり，燃料ガス，原料ガスとしての利用が期待できる。Fig. 7にガス化温度を1000℃として酸素濃度を変えた場合の生成ガス組成，C_GおよびH_hの変化を示す。酸素濃度の増加と共にCO_2は減少し，CO，H_2合わせて70%となった。Fig. 8はアッシュホッパーおよび集塵器で補集した粒子中に含まれる灰分割合とガス化温度との関係を示したもので補集ダストの灰分は80数%であり，溢流ガス化灰粒子の灰分はガス化温度が1000℃を越えると95～99%となった。この粒子は再び液化残渣と混合して使用することができる。フレークピッチのハイブリッド粒子についてのガス化実験結果をFigs. 9,10に示す。遠心分離機残渣の場合より反応性がよく，C_Gはほぼ100%となった。生成ガス組成のガス化温度，酸素濃度に対する変化は遠心分離機残渣の場合と同じであった。生成ガス中のH_2Sは0.03～0.37%であった。なお，高圧流動層石炭ガス化プロセスのサイクロンダスト（表面積280m²／g，平均粒径0.1㎜）と液化残渣とによるハイブリッド粒子化も可能であり，検討中である。

謝　辞

本研究に使用した液化残渣は新エネルギー開発機構（NEDO）を通じて日本鋼管㈱から提供して頂きました。また本稿をまとめるにあたり，北海道大学工学部千葉忠俊助教授に有益な御助言を頂きました。併せて謝意を表します。

Nomenclature

C_G＝carbon conversion 〔－〕

H_h＝heating value of produced gas〔MJ/Nm³〕

U_{mf}＝minimum fluidization velocity 〔m／s〕

＊化学工学論文集　第13巻第15号（1987）より転載

Table 1 Analysis of hybrid particles

Ultimate [wt %]	Hybrid cen. residue	Hybrid pitch
C	36.72	54.77
H	2.05	1.98
O	4.31	3.50
N	0.42	0.80
S	1.09	0.31
Ash	55.41	39.41
Heating value [MJ/kg]	14.69	21.31
ρ_b [kg/m^3]	620	530
U_{mf} [m/s]	0.36	0.24

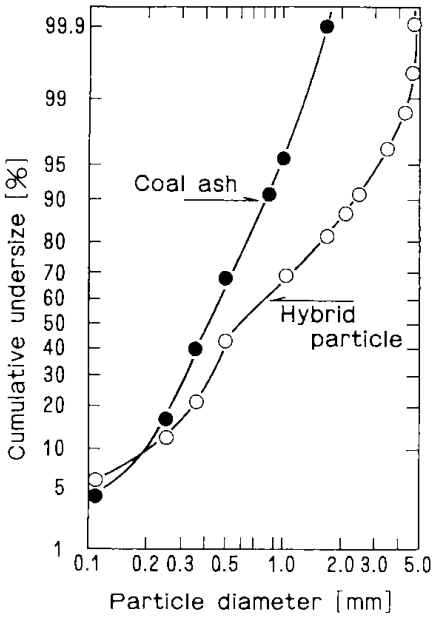

Fig. 4 Size distribution of coal ash and hybrid particles of ash and centrifuge residue

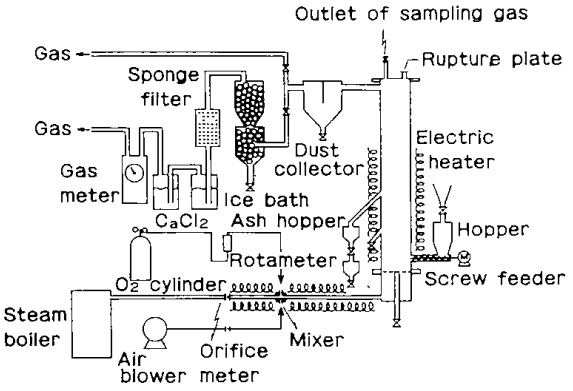

Fig. 5 Schematic diagram of experimental apparatus

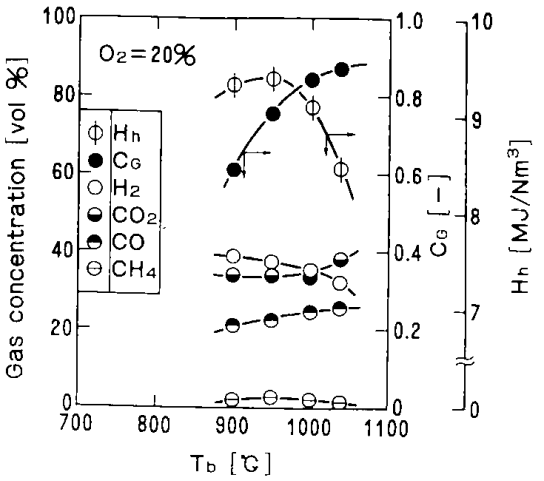

Fig. 6 Effect of bed temperature on gas concentration of product gas and on carbon conversion for the hybrid particles of centrifuge residue

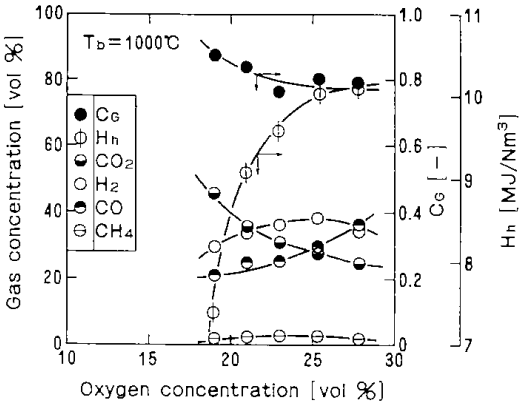

Fig. 7 Effect of oxygen % on gas concentration of product gas and on carbon conversion for the hybrid particles of centrifuge residue

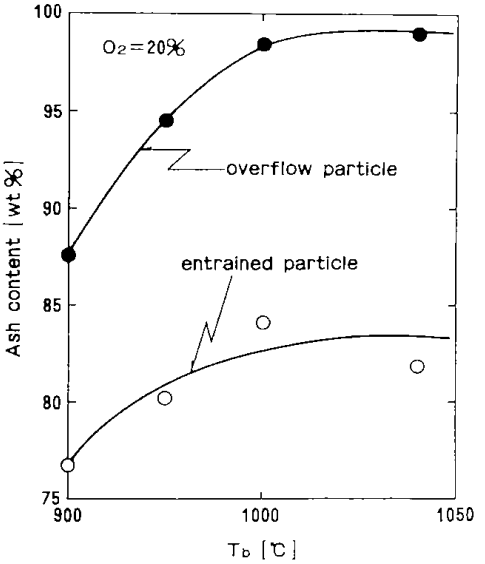

Fig. 8 Effect of bed temperature on ash content for the hybrid particles of centrifuge residue

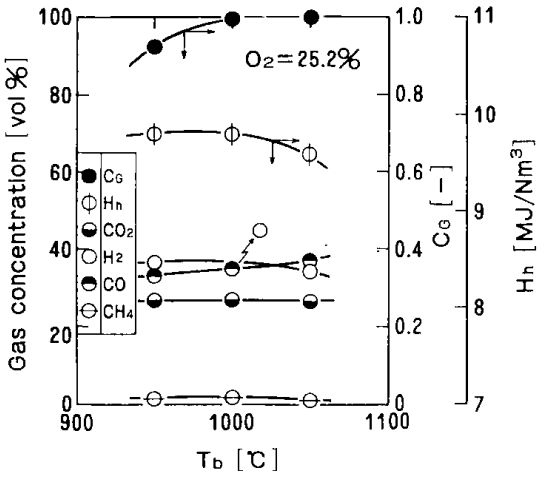

Fig. 9 Effect of bed temperature on gas concentration of product gas and on carbon conversion for the hybrid particles of flake pitch

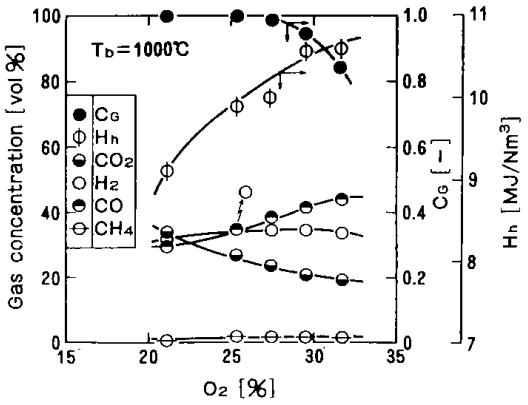

Fig. 10 Effect of oxygen % on gas concentration of product gas and on carbon conversion for the hybrid particles of flake pitch

Gasification of Hybrid Particles of Gasification and Liquefaction Residue of Coal

Yoneshiro Tazaki, Shigeo Chiba, Midori Yumiyama, Shohei Takeda, Senji Honma, Kunihiro Kitano and Junichi Kawabata

Government Industrial Development Laboratory, Hokkaido, Sapporo 004

Key Words: Fluidization, Coal Gasification, Coal Liquefaction, Residue, Hybrid

Hybrid particles of coal ash from gasifier and higher viscous residue and solid pitch from coal liquefaction were successfully produced by two new methods. They were then gasified by stean and oxygen in a fluidized bed under atmospheric pressure. Gasification characteristics of these particles, such as the distribution and yield of gas produced and the carbon conversion, were evaluated as a function of operating variables.

北海道工業開発試験所報告
第 46 号

昭和63年3月25日　印刷
昭和63年3月25日　発行

発　行　所　工業技術院北海道工業開発試験所
札幌市豊平区月寒東2条17丁目2番1号
電　話　011 (851) 0151 (代)
印　刷　所　東日本印刷株式会社
札幌市中央区南6条西17丁目
電　話　011 (551) 1120 (代)

REPORTS OF THE GOVERNMENT INDUSTRIAL DEVEROPMENT LABORATORY, HOKKAIDO

Contents

Published by

The Government Industrial Development Laboratory, I
The Government Industrial Development Laboratory, Hokkaido
2Jo 17Chome, Tsukisamu-Iligashi, Toyohiraku, Sapporo, Japan